



ORIGINAL ARTICLE

Hossein B. Khaniki · Mergen H. Ghayesh · Rey Chin ·
Shahid Hussain

Internal resonance and bending analysis of thick visco-hyper-elastic arches

Received: 9 June 2022 / Accepted: 19 October 2022 / Published online: 23 November 2022
© The Author(s) 2022

Abstract In this study, a comprehensive analysis of visco-hyper-elastic thick soft arches under an external time-independent as well as time-dependent loads is presented from bending and internal resonance phenomenon perspectives. Axial, transverse and rotation motions are considered for modelling the thick and soft arch in the framework of the Mooney–Rivlin and Kelvin–Voigt visco-hyper-elastic schemes and third-order shear deformable models. The arch is assumed to be incompressible and is modelled using von Kármán geometric nonlinearity in the strain–displacement relationship. Using a virtual work method, the bending equations are derived. For the vibration analysis, three, coupled, highly nonlinear equations of motions are obtained using force-moment balance method. The Newton–Raphson method together with the dynamic equilibrium technique is used for the bending and vibration analyses. A detailed study on the influence of having visco-hyper-elasticity and arch curvature in the frequency response of the system is given in detail, and the bending deformation due to the applied static load is presented. The influence of having thick, soft arches with different slenderness ratios is shown, and the forced vibration response is discussed. Moreover, internal resonance in the system is studied showing that the curvature term in the structure can lead to three-to-one internal resonances, showing a rich nonlinear frequency response. The results of this study are a step forward in studying the visco-hyper-elastic behaviour of biological structures and soft tissues.

Keywords Internal resonance · Visco-elastic · Visco-hyper-elastic · Arch · Mooney–Rivlin · Kelvin–Voigt · Bending · Nonlinear vibration

1 Introduction

Arches are one of the main curved structures used in different engineering applications including civil and mechanical engineering. In civil engineering, arches have been employed for different construction purposes such as bridges and subway stations [1, 2] as it can carry greater loads compared to straight structures. As an application in the field of mechanical engineering, arch structures have been used in designing different types of energy harvesters to optimise the efficiency of the system [3–6]. For instance, in a study presented by Yang

Communicated by Andreas Öchsner.

H. B. Khaniki (✉) · M. H. Ghayesh (✉) · R. Chin
School of Mechanical Engineering, University of Adelaide, Adelaide, South Australia 5005, Australia
E-mail: hossein.bakhshikhaniki@adelaide.edu

M. H. Ghayesh
E-mail: mergen.ghayesh@adelaide.edu.au

S. Hussain
Faculty of Science and Technology, University of Canberra, Canberra, Australia

et al. [7], it was shown that by using arch structures, the total harvested power was 200% times more power compared to straight structures. As another example, shallow arches have also been used and examined for microelectromechanical systems (MEMS) [8].

During the last few years, researchers have studied the mechanical behaviour of both flat structures (including beams and plates) [9–15] and curved structures (including shells and arches) [16–23] to be able to use them efficiently for specific purposes. Focusing on arch structures, their behaviour in different engineering conditions has been examined lately. To name a few, Yang et al. [24] reinforced elastic arch structures using graphene nanoplatelets and studied the linear vibration behaviour of graphene-reinforced arches. Different fibre distribution was modelled using Halpin–Tsai micromechanics model and Hamilton’s principle showing that out-of-plane and in-plane linear frequencies of the elastic arch are highly affected by the fibre distribution and percentage. For dynamic instability analysis, Zhao et al. [25] studied the influence of having porosity in modelling graphene-reinforced elastic arches; it was shown that the best dynamic instability resistance can be seen in the symmetric porosity distribution model. The nonlinear mechanics of elastic shallow arches with nonuniform cross section made of functionally graded materials (FGMs) have been investigated by Ghayesh and Farokhi [26]. Coupled axial-transverse equations of motion were obtained using Euler-Bernoulli theory and Hamilton’s principle; it was shown that as the arch curvature increases, the maximum amplitude of transverse vibration decreases. For MEMS structures, Farokhi et al. [27] studied the pull-in phenomena in micro-scale arch structures. Using a high-dimensional reduced-order Galerkin model and generalised Hamilton’s principle, it was shown that by increasing the curvature of the arch, the DC voltage for pull-in phenomena increases.

The previous studies were mainly focused on linear-elastic structures under small strains. However, soft materials undergo large strains, which makes the classic linear modelling of the behaviour inaccurate for many hyper-elastic structures. There has been a significant attention on hyper-elastic structures in the past few years focusing on the statics [28–31] and dynamics [32–35]. In some recent studies, the anti-clastic bending of hyper-elastic beams in finite elasticity has been investigated by Lanzoni and Tarantino [36–38]. Khaniki et al. [39,40] have examined the nonlinear vibration and mechanics of axially moving hyper-elastic structures and layered hyper-elastic beams. In another study, Khaniki et al. [41] investigated the effect of having porosity in hyper-elastic structures providing a porous-hyper-elastic strain energy model and modelling the vibration behaviour of porous soft beams. A detailed review on the nonlinear dynamic behaviour of different hyper-elastic structures can be found in Ref. [42].

However, since some soft structures show a combination of viscoelasticity and hyper-elasticity, researchers have developed different models for such structures [43–47]. In a recent study presented by Li et al. [48], a wide range of visco-hyper-elastic constitutive models were developed. The viscoelasticity was modelled via Maxwell and Kelvin–Voigt models, and the hyper-elasticity was modelled via neo-Hookean, Mooney–Rivlin, and Ogden models. It was shown that the proposed models are capable of modelling both hyper-elasticity and viscoelasticity of the biological structure. Since visco-hyper-elastic structures are widely applicable for modelling human body organs, soft robots and prosthesis, the visco-hyper-elastic constitutive models are useful for studying and manufacturing accurate mechanical and biomechanical structures in different environments.

Besides, since most of the hyper-elastic structures are significantly softer than linear-elastic structures, it is very likely to have them bent (like arches and shells) in real-life applications. Accordingly, in this study, *visco-hyper-elastic* thick soft shallow arches are examined in the framework of nonlinear bending and vibrations (with and without internal resonances). Since the soft arch is assumed to be thick, a third-order shear deformable theory is used and the visco-hyper-elasticity is modelled following Ref. [48] by using Mooney–Rivlin and Kelvin–Voigt models. The bending behaviour of the soft arch is formulated using the virtual work method and solved using the Newton–Raphson method. For the vibration analysis, the equations of motion are obtained using the force-moment balance method and solved using a dynamic equilibrium technique. The effect of having curvature in the structure is analysed, and the internal resonance phenomena caused by having this nonlinearity in the system are discussed. A detailed discussion of the influence of curvature term, the slenderness ratio and three-to-one internal resonance is given.

2 Bending of hyper-elastic thick arch formulation

For a thick, soft, shallow arch, using a higher-order shear deformation theory, by considering plane motion, von Kármán’s geometric nonlinearity, and curvature in the thickness direction, the nonlinear *static* strain terms

are obtained as

$$\varepsilon_{11}(x_1, x_3) = \frac{du_1(x_1)}{dx_1} + \frac{1}{2} \left(\frac{du_3(x_1)}{dx_1} \right)^2 + \frac{du_3(x_1)}{dx_1} \frac{du_{30}(x_1)}{dx_1} + x_3 \frac{d\phi(x_1)}{dx_1} + \mathfrak{S}_1 \left[\frac{d^2u_3(x_1)}{dx_1^2} + \frac{d\phi(x_1)}{dx_1} \right], \quad (1)$$

$$\varepsilon_{13}(x_1) = \mathfrak{S}_2 \left(\frac{du_3(x_1)}{dx_1} + \phi(x_1) \right), \quad (2)$$

$$\varepsilon_{33} \neq 0 \quad (\text{should satisfy the incompressibility condition}) \quad (3)$$

with

$$\mathfrak{S}_1 = -\frac{4x_3^3}{3h^2}, \quad \mathfrak{S}_2 = \frac{1}{2} \left(1 - 4\frac{x_3^2}{h^2} \right), \quad (4)$$

where u_1 and u_3 are the displacements of the arch in the x_1 and x_3 directions (shown in Fig. 1a), u_{30} is the curvature of the shallow arch, ε_{11} and ε_{33} are the axial strains in the x_1 and x_3 directions and ε_{13} is the shear strain. By considering plane motion and incompressible material, the right Cauchy-Green strain tensor is written as [49]

$$C = \begin{bmatrix} (1 + \varepsilon_{11})^2 + \varepsilon_{13}^2 & 0 & \varepsilon_{11}\varepsilon_{13} + 2\varepsilon_{13} + \varepsilon_{33}\varepsilon_{13} \\ 0 & 1 & 0 \\ \varepsilon_{11}\varepsilon_{13} + 2\varepsilon_{13} + \varepsilon_{33}\varepsilon_{13} & 0 & (1 + \varepsilon_{33})^2 + \varepsilon_{13}^2 \end{bmatrix}, \quad (5)$$

which contains nonlinear higher-order strain terms since *hyper-elastic* structures undergo large strains and cannot be modelled by considering the linear part alone, as is undertaken for *elastic* structures.

The principle of virtual work is not only for linear elastic structures and can be applied for hyper-elastic structures [50]. To this end, by using the Mooney–Rivlin hyper-elastic strain energy density [51,52] and the principle of virtual work, the variation of the energy term, due to the static applied forces, can be written in three variation terms for axial (*PE1*), transverse (*PE2*) and rotation (*PE3*) variations as

$$\int_0^L [F_{s1}\delta u_1 + F_{s3}\delta u_3 + F_{s2}\delta\phi] dx_1 = \int_0^L [(PE1)\delta u_1 + (PE2)\delta u_3 + (PE3)\delta\phi] dx_1, \quad (6)$$

where *PE1*, *PE2*, *PE3* are given in Appendix A for the sake of brevity, with the moment of area coefficients defined as

$$\begin{aligned} I_{00} &= \int_A 1 dA, & I_{11} &= \int_A u_3 dA, & I_{22} &= \int_A \mathfrak{S}_1 dA, & I_{33} &= \int_A (u_3 + \mathfrak{S}_1) dA, \\ I_{44} &= \int_A \mathfrak{S}_1^2 dA, & I_{55} &= \int_A \mathfrak{S}_2^2 dA, \\ I_{66} &= \int_A \mathfrak{S}_1 (u_3 + \mathfrak{S}_1) dA, & I_{77} &= \int_A (1 - \mathfrak{S}_2^2) dA, \\ I_{88} &= \int_A (1 - 2\mathfrak{S}_2^2) dA, & I_{99} &= \int_A (\mathfrak{S}_1 + u_3)^2 dA, \\ I_{1010} &= \int_A \mathfrak{S}_1^3 dA, & I_{1111} &= \int_A \mathfrak{S}_1 \mathfrak{S}_2^2 dA, & I_{1212} &= \int_A \mathfrak{S}_1 (1 - \mathfrak{S}_2^2) dA, & I_{1313} &= \int_A \mathfrak{S}_2^2 (\mathfrak{S}_1 + u_3) dA, \\ I_{1414} &= \int_A \mathfrak{S}_1^2 (\mathfrak{S}_1 + u_3) dA, & I_{1515} &= \int_A \mathfrak{S}_1 (\mathfrak{S}_1 + u_3)^2 dA, & I_{1616} &= \int_A (\mathfrak{S}_1 + u_3)^3 dA, \end{aligned}$$

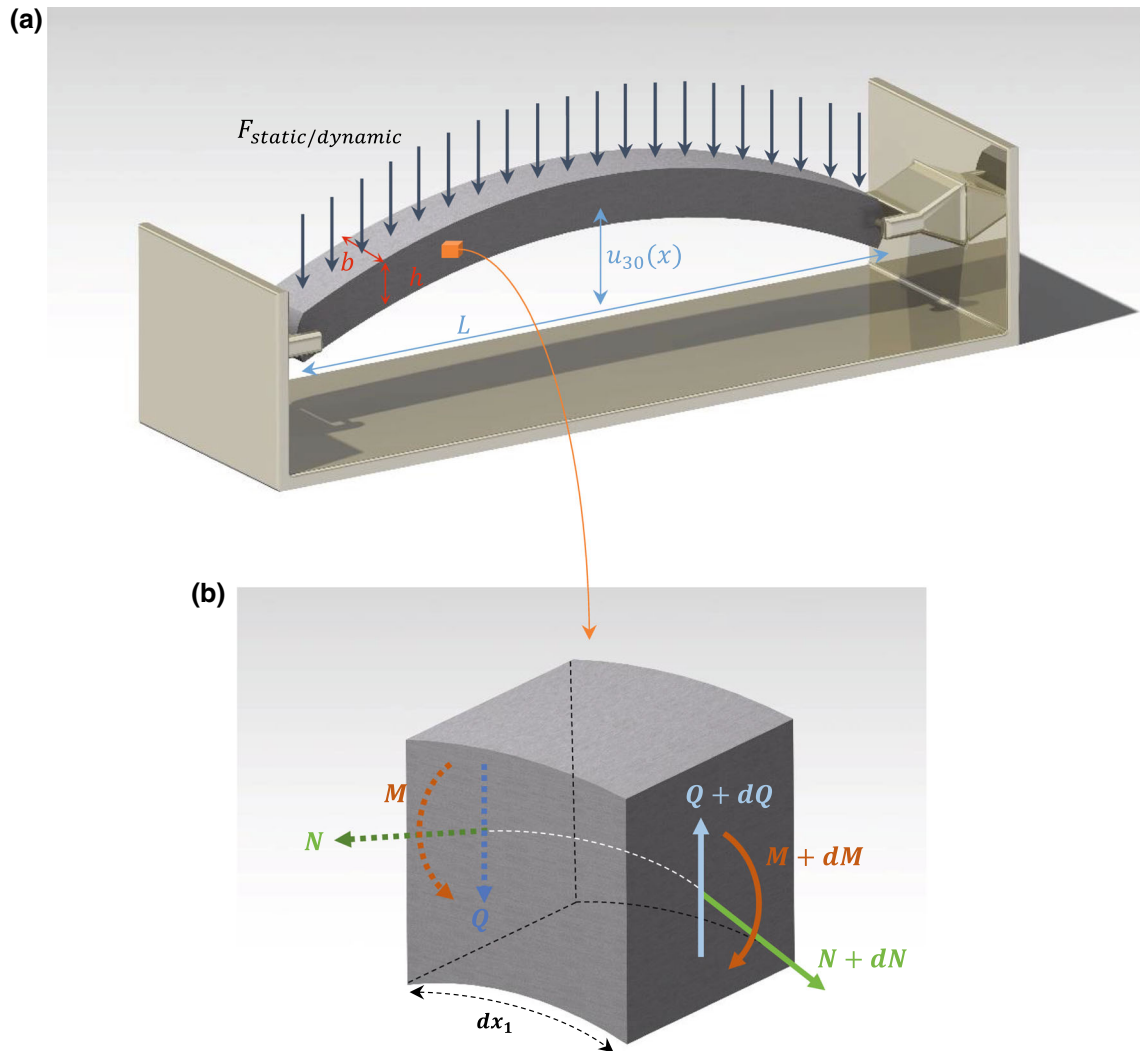


Fig. 1 Schematic figure of a visco-hyper-elastic thick shallow arch with simply supported boundary conditions

$$I_{1717} = \int_A u_3 (u_3 + \mathfrak{S}_1) \mathfrak{S}_2^2 dA, \quad I_{1818} = \int_A \mathfrak{S}_2^3 dA, \quad I_{1919} = \int_A (u_3 + \mathfrak{S}_1) (\mathfrak{S}_2^2 - 1) dA. \quad (7)$$

Using Eqs. (1–7), three equilibrium equations for the bending analysis are obtained by having homogeneity in the arch as

$$\begin{aligned} & -8C_T I_{00} u_{1x_1x_1} - 8C_T I_{00} \frac{d}{dx_1} (u_{3x_1} u_{30x_1}) + 12C_T I_{00} \frac{d}{dx_1} (u_{1x_1}^2) + 24C_T I_{00} \frac{d}{dx_1} (u_{1x_1} u_{3x_1} u_{30x_1}) \\ & - 4C_T I_{77} \frac{d}{dx_1} (u_{3x_1}^2) + 12C_T I_{00} \frac{d}{dx_1} (u_{3x_1}^2 u_{30x_1}^2) + 12C_T I_{44} \frac{d}{dx_1} (u_{3x_1x_1}^2) \\ & + 24C_T I_{66} \frac{d}{dx_1} (u_{3x_1x_1} \phi_{x_1}) + 8C_T I_{55} \frac{d}{dx_1} (u_{3x_1} \phi) + 12C_T I_{99} \frac{d}{dx_1} (\phi_{x_1}^2) + 4C_T I_{55} \frac{d}{dx_1} (\phi^2) \\ & + 12C_T I_{00} \frac{d}{dx_1} (u_{1x_1} u_{3x_1}^2) + 12C_T I_{00} \frac{d}{dx_1} (u_{30x_1} u_{3x_1}^3) + 3C_T I_{00} \frac{d}{dx_1} (u_{3x_1}^4) = F_{S1}, \quad (8) \\ & -8C_T I_{66} u_{3x_1x_1x_1} + 8C_T I_{55} u_{3x_1} - 8C_T I_{99} \phi_{x_1x_1} + 8C_T I_{55} \phi + 24C_T I_{66} \frac{d}{dx_1} (u_{1x_1} u_{3x_1x_1}) - 8C_T I_{55} u_{1x_1} u_{3x_1} \end{aligned}$$

$$\begin{aligned}
& +24C_T I_{99} \frac{d}{dx_1} (u_{1x_1} \phi_{x_1}) - 8C_T I_{55} u_{1x_1} \phi + 24C_T I_{66} \frac{d}{dx_1} (u_{3x_1} u_{3x_1 x_1} u_{30x_1}) - 8C_T I_{55} u_{3x_1}^2 u_{30x_1} \\
& +24C_T I_{99} \frac{d}{dx_1} (u_{3x_1} \phi_{x_1} u_{30x_1}) - 8C_T I_{55} u_{3x_1} \phi u_{30x_1} + 12C_T I_{66} \frac{d}{dx_1} (u_{3x_1}^2 u_{3x_1 x_1}) - 4C_T I_{55} u_{3x_1}^3 \\
& +12C_T I_{99} \frac{d}{dx_1} (u_{3x_1}^2 \phi_{x_1}) - 4C_T I_{55} u_{3x_1}^2 \phi = F_{S2}. \tag{9} \\
& -8C_T I_{00} \frac{d}{dx_1} (u_{1x_1} u_{30x_1}) - 8C_T I_{00} \frac{d}{dx_1} (u_{3x_1} u_{30x_1}^2) \\
& +8C_T I_{44} u_{3x_1 x_1 x_1 x_1} - 8C_T I_{55} u_{3x_1 x_1} + 8C_T I_{66} \phi_{x_1 x_1 x_1} - 8C_T I_{55} \phi_{x_1} \\
& +12C_T I_{00} \frac{d}{dx_1} (u_{1x_1}^2 u_{30x_1}) - 8C_T I_{77} \frac{d}{dx_1} (u_{1x_1} u_{3x_1}) \\
& +24C_T I_{00} \frac{d}{dx_1} (u_{1x_1} u_{3x_1} u_{30x_1}^2) - 24C_T I_{44} \frac{d^2}{dx_1^2} (u_{1x_1} u_{3x_1 x_1}) \\
& -24C_T I_{66} \frac{d^2}{dx_1^2} (u_{1x_1} \phi_{x_1}) + 8C_T I_{55} \frac{d}{dx_1} (u_{1x_1} \phi) \\
& -12C_T I_{77} \frac{d}{dx_1} (u_{3x_1}^2 u_{30x_1}) + 12C_T I_{00} \frac{d}{dx_1} (u_{3x_1}^2 u_{30x_1}^3) \\
& +12C_T I_{44} \frac{d}{dx_1} (u_{3x_1}^2 u_{30x_1}) - 24C_T I_{44} \frac{d^2}{dx_1^2} (u_{3x_1} u_{3x_1 x_1} u_{30x_1}) + 24C_T I_{66} \frac{d}{dx_1} (u_{3x_1 x_1} \phi_{x_1} u_{30x_1}) \\
& +16C_T I_{55} \frac{d}{dx_1} (u_{3x_1} \phi u_{30x_1}) - 24C_T I_{66} \frac{d^2}{dx_1^2} (u_{3x_1} \phi_{x_1} u_{30x_1}) \\
& +12C_T I_{99} \frac{d}{dx_1} (\phi_{x_1}^2 u_{30x_1}) + 4C_T I_{55} \frac{d}{dx_1} (\phi^2 u_{30x_1}) \\
& +12C_T I_{00} \frac{d}{dx_1} (u_{1x_1}^2 u_{3x_1}) + 36C_T I_{00} \frac{d}{dx_1} (u_{1x_1} u_{3x_1}^2 u_{30x_1}) \\
& -4C_T I_{88} \frac{d}{dx_1} (u_{3x_1}^3) + 24C_T I_{00} \frac{d}{dx_1} (u_{3x_1}^3 u_{30x_1}^2) \\
& +12C_T I_{44} \frac{d}{dx_1} (u_{3x_1} u_{3x_1 x_1}^2) - 12C_T I_{44} \frac{d^2}{dx_1^2} (u_{3x_1}^2 u_{3x_1 x_1}) \\
& +24C_T I_{66} \frac{d}{dx_1} (u_{3x_1} u_{3x_1 x_1} \phi_{x_1}) + 12C_T I_{55} \frac{d}{dx_1} (u_{3x_1}^2 \phi) \\
& -12C_T I_{66} \frac{d^2}{dx_1^2} (u_{3x_1}^2 \phi_{x_1}) + 12C_T I_{99} \frac{d}{dx_1} (u_{3x_1} \phi_{x_1}^2) + 4C_T I_{55} \frac{d}{dx_1} (u_{3x_1} \phi^2) + 12C_T I_{00} \frac{d}{dx_1} (u_{1x_1} u_{3x_1}^3) \\
& +15C_T I_{00} \frac{d}{dx_1} (u_{30x_1} u_{3x_1}^4) + 3C_T I_{00} \frac{d}{dx_1} (u_{3x_1}^5) = F_{S3}, \tag{10}
\end{aligned}$$

It can be seen that the equilibrium equations are highly nonlinear in hyper-elasticity terms, with a high coupling between the axial, rotation and transverse motions. The equilibrium equations can be validated by comparing them to those presented in Ref. [40] by neglecting the curvature terms from these equations and unsymmetrical and time-dependant terms in the equations of motion of Ref. [40]. By employing the solution procedure given in Sect. 4, the bending behaviour of soft thick shallow arches will be obtained.

3 Dynamics of visco-hyper-elastic thick arch formulation via force-moment balance method

For the time-dependent analysis and modelling of soft thick shallow arches, using the same assumptions given in Sect. 2, the nonlinear strain terms are written as

$$\varepsilon_{11}(x_1, x_3, t) = \frac{\partial u_1(x_1, t)}{\partial x_1} + \frac{1}{2} \left(\frac{\partial u_3(x_1, t)}{\partial x_1} \right)^2 + \frac{\partial u_3(x_1, t)}{\partial x_1} \frac{du_{30}(x_1)}{dx_1}$$

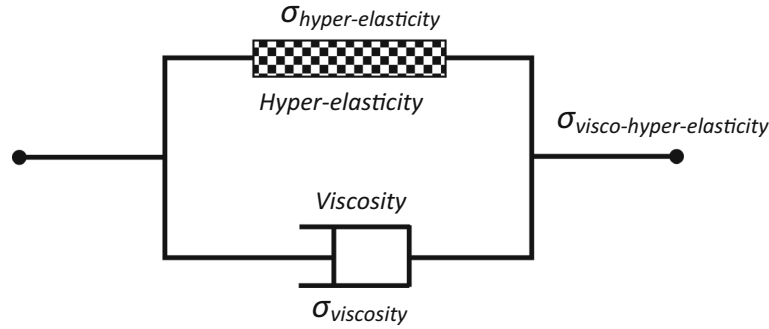


Fig. 2 Constitutive model of Kelvin–Voigt visco-hyper-elasticity

$$+x_3 \frac{\partial \phi(x_1, t)}{\partial x_1} + \mathfrak{S}_1 \left[\frac{\partial^2 u_3(x_1, t)}{\partial x_1^2} + \frac{\partial \phi(x_1, t)}{\partial x_1} \right], \quad (11)$$

$$\varepsilon_{13}(x_1, t) = \mathfrak{S}_2 \left(\frac{\partial u_3(x_1, t)}{\partial x_1} + \phi(x_1, t) \right), \quad (12)$$

$$\varepsilon_{33} \neq 0 \quad (\text{should satisfy the incompressibility condition}). \quad (13)$$

For visco-hyper-elastic structures, Li et al. [48] have shown that the visco-hyper Kelvin–Voigt model has a good accuracy in modelling visco-hyper-elastic structures while using Mooney–Rivlin, neo-Hookean and Ogden strain energy density models. The visco-hyper-elastic model (Fig. 2) is presented as [48]

$$\sigma_{\text{visco-hyper}} = \sigma_{\text{hyperelastic}} + \xi_k \dot{\varepsilon}, \quad (14)$$

(Talk about the feasible applicability of the approach) For an element of the thick visco-hyper-elastic arch, shown in Fig. 2b, Newton’s law is applied for the rotational motion, as well as translational ones by having [53]

$$\frac{\partial N(x_1, x_3, t)}{\partial x_1} = -\rho I_{00} u_{1tt} - \rho I_{22} u_{3xxt} - \rho I_{33} \phi_{tt}, \quad (15)$$

$$\frac{\partial Q(x_1, x_3, t)}{\partial x_1} + F_{\text{external}}(x_1, x_3, t) = \rho I_{22} u_{1xtt} + \rho I_{44} u_{3xxt} + \rho I_{66} \phi_{xtt} - \rho I_{00} u_{3tt}, \quad (16)$$

$$\frac{\partial M(x_1, x_3, t)}{\partial x_1} - Q(x_1, x_3, t) = -\rho I_{33} u_{1tt} - \rho I_{66} u_{3xxt} - \rho I_{99} \phi_{tt}, \quad (17)$$

where the stress resultants are defined as [54]

$$N = \int_A \sigma_{\text{visco-hyper}, x_1 x_1} dA, \quad (18)$$

$$M = \int_A x_3 \sigma_{\text{visco-hyper}, x_1 x_1} dA, \quad (19)$$

$$Q = \int_A \sigma_{\text{visco-hyper}, x_1 x_3} dA, \quad (20)$$

and the applied external periodic load with the magnitude of F is given as

$$F_{\text{external}} = F \cos(\omega t). \quad (21)$$

For isotropic visco-hyper-elastic shallow arches, by using force-moment balance method, one can reach the coupled equations of motions which are shown in Appendix B for the sake of brevity. By neglecting the viscoelasticity and the arch-related terms, the equations of motion can be validated through Ref. [40]. It can be seen that all three equations of motion are highly nonlinear in visco-elasticity and hyper-elasticity terms, with a high coupling between the axial, rotation and transverse motions. By using the solution procedure given in Sect. 5, the vibration behaviour of soft thick shallow arches will be obtained.

4 Solution procedure for hyper-elastic bending analysis

By assuming only transverse external load on the system ($F_{S1} = F_{S2} = 0$ and $F_{S3} = F$) and defining nondimensional terms as

$$\begin{aligned} x_1^* &= \frac{x_1}{L}, \quad u_1^* = \frac{u_1}{h}, \quad u_3^* = \frac{u_3}{h}, \quad u_{30}^* = \frac{u_{30}}{h}, \quad I_{00}^* = \frac{I_{00}h^2}{I_{44}}, \\ I_{55}^* &= \frac{I_{55}h^2}{I_{44}}, \quad I_{66}^* = \frac{I_{66}}{I_{44}}, \quad I_{77}^* = \frac{I_{77}h^2}{I_{44}}, \\ I_{88}^* &= \frac{I_{88}h^2}{I_{44}}, \quad I_{99}^* = \frac{I_{99}}{I_{44}}, \quad \eta = \frac{h}{L}, \quad F^* = \frac{FL^4}{C_T I_{44}h}, \end{aligned} \quad (22)$$

the nondimensional equilibrium equations are written as

$$\begin{aligned} & -8I_{00} \frac{1}{\eta^2} u_{1x_1x_1} - 8I_{00} \frac{1}{\eta} \frac{d}{dx_1} (u_{3x_1} u_{30x_1}) \\ & + 12I_{00} \frac{1}{\eta} \frac{d}{dx_1} (u_{1x_1}^2) + 24I_{00} \frac{d}{dx_1} (u_{1x_1} u_{3x_1} u_{30x_1}) - 4I_{77} \frac{1}{\eta} \frac{d}{dx_1} (u_{3x_1}^2) + 12I_{00} \eta \frac{d}{dx_1} (u_{3x_1}^2 u_{30x_1}^2) \\ & + 12\eta \frac{d}{dx_1} (u_{3x_1x_1}^2) + 24I_{66} \frac{d}{dx_1} (u_{3x_1x_1} \phi_{x_1}) + 8I_{55} \frac{1}{\eta^2} \frac{d}{dx_1} (u_{3x_1} \phi) + 12I_{99} \frac{1}{\eta} \frac{d}{dx_1} (\phi_{x_1}^2) + 4I_{55} \frac{1}{\eta^3} \frac{d}{dx_1} (\phi^2) \\ & + 12I_{00} \frac{d}{dx_1} (u_{1x_1} u_{3x_1}^2) + 12I_{00} \eta \frac{d}{dx_1} (u_{30x_1} u_{3x_1}^3) + 3I_{00} \eta \frac{d}{dx_1} (u_{3x_1}^4) = 0, \quad (23) \\ & -8I_{00} \frac{1}{\eta} \frac{d}{dx_1} (u_{1x_1} u_{30x_1}) - 8I_{00} \frac{d}{dx_1} (u_{3x_1} u_{30x_1}^2) + 8u_{3x_1x_1x_1x_1} - 8I_{55} \frac{1}{\eta^2} u_{3x_1x_1} + 8I_{66} \frac{1}{\eta} \phi_{x_1x_1x_1} - 8I_{55} \frac{1}{\eta^3} \phi_{x_1} \\ & + 12I_{00} \frac{d}{dx_1} (u_{1x_1}^2 u_{30x_1}) - 8I_{77} \frac{1}{\eta} \frac{d}{dx_1} (u_{1x_1} u_{3x_1}) + 24I_{00} \eta \frac{d}{dx_1} (u_{1x_1} u_{3x_1} u_{30x_1}^2) - 24\eta \frac{d^2}{dx_1^2} (u_{1x_1} u_{3x_1x_1}) \\ & - 24I_{66} \frac{d^2}{dx_1^2} (u_{1x_1} \phi_{x_1}) + 8I_{55} \frac{1}{\eta^2} \frac{d}{dx_1} (u_{1x_1} \phi) - 12I_{77} \frac{d}{dx_1} (u_{3x_1}^2 u_{30x_1}) + 12I_{00} \eta^2 \frac{d}{dx_1} (u_{3x_1}^2 u_{30x_1}^3) \\ & + 12\eta^2 \frac{d}{dx_1} (u_{3x_1x_1}^2 u_{30x_1}) - 24\eta^2 \frac{d^2}{dx_1^2} (u_{3x_1} u_{3x_1x_1} u_{30x_1}) + 24I_{66} \eta \frac{d}{dx_1} (u_{3x_1x_1} \phi_{x_1} u_{30x_1}) \\ & + 16I_{55} \frac{1}{\eta} \frac{d}{dx_1} (u_{3x_1} \phi u_{30x_1}) - 24I_{66} \eta \frac{d^2}{dx_1^2} (u_{3x_1} \phi_{x_1} u_{30x_1}) + 12I_{99} \frac{d}{dx_1} (\phi_{x_1}^2 u_{30x_1}) \\ & + 4I_{55} \frac{1}{\eta^2} \frac{d}{dx_1} (\phi^2 u_{30x_1}) + 12I_{00} \frac{d}{dx_1} (u_{1x_1}^2 u_{3x_1}) + 36I_{00} \eta \frac{d}{dx_1} (u_{1x_1} u_{3x_1}^2 u_{30x_1}) - 4I_{88} \frac{d}{dx_1} (u_{3x_1}^3) \\ & + 24I_{00} \frac{d}{dx_1} (u_{3x_1}^3 u_{30x_1}^2) + 12\eta^2 \frac{d}{dx_1} (u_{3x_1} u_{3x_1x_1}^2) - 12\eta^2 \frac{d^2}{dx_1^2} (u_{3x_1}^2 u_{3x_1x_1}) \\ & + 24I_{66} \eta \frac{d}{dx_1} (u_{3x_1} u_{3x_1x_1} \phi_{x_1}) + 12I_{55} \frac{1}{\eta} \frac{d}{dx_1} (u_{3x_1}^2 \phi) - 12I_{66} \eta \frac{d^2}{dx_1^2} (u_{3x_1}^2 \phi_{x_1}) \\ & + 12I_{99} \frac{d}{dx_1} (u_{3x_1} \phi_{x_1}^2) + 4I_{55} \frac{1}{\eta^2} \frac{d}{dx_1} (u_{3x_1} \phi^2) + 12I_{00} \eta \frac{d}{dx_1} (u_{1x_1} u_{3x_1}^3) + 15I_{00} \eta^2 \frac{d}{dx_1} (u_{30x_1} u_{3x_1}^4) \\ & + 3I_{00} \eta^2 \frac{d}{dx_1} (u_{3x_1}^5) = F, \quad (24) \\ & -8I_{66} \eta u_{3x_1x_1x_1} + 8I_{55} \frac{1}{\eta} u_{3x_1} - 8I_{99} \phi_{x_1x_1} + 8I_{55} \frac{1}{\eta^2} \phi + 24I_{66} \eta^2 \frac{d}{dx_1} (u_{1x_1} u_{3x_1x_1}) - 8I_{55} u_{1x_1} u_{3x_1} \\ & + 24I_{99} \eta \frac{d}{dx_1} (u_{1x_1} \phi_{x_1}) - 8I_{55} \frac{1}{\eta} u_{1x_1} \phi + 24I_{66} \eta^3 \frac{d}{dx_1} (u_{3x_1} u_{3x_1x_1} u_{30x_1}) - 8I_{55} \eta u_{3x_1}^2 u_{30x_1} \\ & + 24I_{99} \eta^2 \frac{d}{dx_1} (u_{3x_1} \phi_{x_1} u_{30x_1}) - 8I_{55} u_{3x_1} \phi u_{30x_1} + 12I_{66} \eta^3 \frac{d}{dx_1} (u_{3x_1}^2 u_{3x_1x_1}) - 4I_{55} \eta u_{3x_1}^3 \\ & + 12I_{99} \eta^2 \frac{d}{dx_1} (u_{3x_1}^2 \phi_{x_1}) - 4I_{55} u_{3x_1}^2 \phi = 0. \quad (25) \end{aligned}$$

where * is neglected from the parameters for the sake of brevity. By employing a series expansion, the degrees of freedom are written as

$$u_1(x_1) = \sum_{j=1}^M \mathfrak{R}_j U_j(x_1), \quad (26)$$

$$u_3(x_1) = \sum_{i=1}^N \mathfrak{N}_i W_i(x_1), \quad (27)$$

$$\phi(x_1) = \sum_{i=1}^N \kappa_i \psi_i(x_1), \quad (28)$$

$$u_{30}(x_1) = W_0(x_1), \quad (29)$$

and the equations of motion are discretised as

$$K_{11}^L \mathfrak{R} + K_{12}^L \mathfrak{N} + K_{11}^{NL} \mathfrak{R}^2 + K_{12}^{NL} \mathfrak{R} \mathfrak{N} + K_{13}^{NL} \mathfrak{N}^2 + K_{14}^{NL} \mathfrak{N} \kappa + K_{15}^{NL} \kappa^2 + K_{16}^{NL} \mathfrak{R} \mathfrak{N}^2 + K_{17}^{NL} \mathfrak{N}^3 + K_{18}^{NL} \mathfrak{N}^4 = 0, \quad (30)$$

$$K_{21}^L \mathfrak{R} + K_{22}^L \mathfrak{N} + K_{22}^L \kappa + K_{21}^{NL} \mathfrak{R}^2 + K_{22}^{NL} \mathfrak{R} \mathfrak{N} + K_{23}^{NL} \mathfrak{R} \kappa + K_{24}^{NL} \mathfrak{N}^2 + K_{25}^{NL} \mathfrak{N} \kappa + K_{26}^{NL} \kappa^2 + K_{27}^{NL} \mathfrak{R}^2 \mathfrak{N} + K_{28}^{NL} \mathfrak{R} \mathfrak{N}^2 + K_{29}^{NL} \mathfrak{N}^3 + K_{210}^{NL} \mathfrak{N}^2 \kappa + K_{211}^{NL} \mathfrak{N} \kappa^2 + K_{212}^{NL} \mathfrak{R} \mathfrak{N}^3 + K_{213}^{NL} \mathfrak{N}^4 + K_{214}^{NL} \mathfrak{N}^5 = F, \quad (31)$$

$$K_{32}^L \mathfrak{N} + K_{33}^L \kappa + K_{31}^{NL} \mathfrak{R} \mathfrak{N} + K_{32}^{NL} \mathfrak{R} \kappa + K_{33}^{NL} \mathfrak{N}^2 + K_{34}^{NL} \mathfrak{N} \kappa + K_{35}^{NL} \mathfrak{N}^3 + K_{36}^{NL} \mathfrak{N}^2 \kappa = 0. \quad (32)$$

The linear stiffness coefficients (K_{ij}^L) of the bending equilibrium equations are defined as

$$K_{11}^L = -8 \frac{1}{\eta^2} I_{00} \int_0^1 U_p(x_1) U_i''(x_1) dx_1, \quad (33)$$

$$K_{12}^L = -8 \frac{1}{\eta} I_{00} \int_0^1 U_p(x_1) \frac{d}{dx_1} (W_i'(x_1) W_0'(x_1)) dx_1, \quad (34)$$

$$K_{21}^L = -8 I_{00} \frac{1}{\eta} \int_0^1 W_l(x_1) \frac{d}{dx_1} (U_i'(x_1) W_0'(x_1)) dx_1, \quad (35)$$

$$K_{22}^L = -8 I_{00} \int_0^1 W_l(x_1) \frac{d}{dx_1} (W_i'(x_1) W_0'^2(x_1)) dx_1 + 8 \int_0^1 W_l(x_1) W_i^{(4)}(x_1) dx_1 - 8 I_{55} \frac{1}{\eta^2} \int_0^1 W_l(x_1) W_i''(x_1) dx_1, \quad (36)$$

$$K_{23}^L = +8 I_{66} \frac{1}{\eta} \int_0^1 W_l(x_1) \psi_i'''(x_1) dx_1 - 8 I_{55} \frac{1}{\eta^3} \int_0^1 W_l(x_1) \psi_i'(x_1) dx_1, \quad (37)$$

$$K_{32}^L = -8 I_{66} \eta \int_0^1 \psi_l(x_1) W_i'''(x_1) dx_1 + 8 I_{55} \frac{1}{\eta} \int_0^1 \psi_l(x_1) W_i'(x_1) dx_1, \quad (38)$$

$$K_{33}^L = +8 I_{55} \frac{1}{\eta^2} \int_0^1 \psi_l(x_1) \psi_i(x_1) dx_1 - 8 I_{99} \int_0^1 \psi_l(x_1) \psi_i''(x_1) dx_1, \quad (39)$$

and the nonlinear stiffness coefficients (K_{ij}^{NL}) are defined as

$$K_{11}^{NL} = +12\frac{1}{\eta}I_{00} \int_0^1 U_p(x_1) \frac{d}{dx_1} \left(U_i'(x_1) U_j'(x_1) \right) dx_1, \quad (40)$$

$$K_{12}^{NL} = +24I_{00} \int_0^1 U_p(x_1) \frac{d}{dx_1} \left(U_i'(x_1) W_j'(x_1) W_0'(x_1) \right) dx_1, \quad (41)$$

$$\begin{aligned} K_{13}^{NL} = & -4\frac{1}{\eta}I_{77} \int_0^1 U_p(x_1) \frac{d}{dx_1} \left(W_i'(x_1) W_j'(x_1) \right) dx_1 \\ & +12\eta I_{00} \int_0^1 U_p(x_1) \frac{d}{dx_1} \left(W_i'(x_1) W_j'(x_1) W_0'^2(x_1) \right) dx_1 \\ & +12\eta \int_0^1 U_p(x_1) \frac{d}{dx_1} \left(W_i''(x_1) W_j''(x_1) \right) dx_1, \end{aligned} \quad (42)$$

$$K_{14}^{NL} = +24I_{66} \int_0^1 U_p(x_1) \frac{d}{dx_1} \left(W_i''(x_1) \psi_j'(x_1) \right) dx_1 + 8\frac{1}{\eta^2}I_{55} \int_0^1 U_p(x_1) \frac{d}{dx_1} \left(W_i'(x_1) \psi_j(x_1) \right) dx_1, \quad (43)$$

$$K_{15}^{NL} = +12\frac{1}{\eta}I_{99} \int_0^1 U_p(x_1) \frac{d}{dx_1} \left(\psi_i'(x_1) \psi_j'(x_1) \right) dx_1 + 4\frac{1}{\eta^3}I_{55} \int_0^1 U_p(x_1) \frac{d}{dx_1} \left(\psi_i(x_1) \psi_j(x_1) \right) dx_1, \quad (44)$$

$$K_{16}^{NL} = +12I_{00} \int_0^1 U_p(x_1) \frac{d}{dx_1} \left(U_i'(x_1) W_j'(x_1) W_k'(x_1) \right) dx_1, \quad (45)$$

$$K_{17}^{NL} = +12\eta I_{00} \int_0^1 U_p(x_1) \frac{d}{dx_1} \left(W_i'(x_1) W_j'(x_1) W_k'(x_1) W_0'(x_1) \right) dx_1, \quad (46)$$

$$K_{18}^{NL} = +3\eta I_{00} \int_0^1 U_p(x_1) \frac{d}{dx_1} \left(W_i'(x_1) W_j'(x_1) W_k'(x_1) W_m'(x_1) \right) dx_1, \quad (47)$$

$$K_{21}^{NL} = +12I_{00} \int_0^1 W_l(x_1) \frac{d}{dx_1} \left(U_i'(x_1) U_j'(x_1) W_0'(x_1) \right) dx_1, \quad (48)$$

$$\begin{aligned} K_{22}^{NL} = & -8I_{77}\frac{1}{\eta} \int_0^1 W_l(x_1) \frac{d}{dx_1} \left(U_i'(x_1) W_j'(x_1) \right) dx_1 - 24\eta \int_0^1 W_l(x_1) \frac{d^2}{dx_1^2} \left(U_i'(x_1) W_j''(x_1) \right) dx_1 \\ & +24I_{00}\eta \int_0^1 W_l(x_1) \frac{d}{dx_1} \left(U_i'(x_1) W_j'(x_1) W_0'^2(x_1) \right) dx_1, \end{aligned} \quad (49)$$

$$K_{23}^{NL} = -24I_{66} \int_0^1 W_l(x_1) \frac{d^2}{dx_1^2} \left(U_i'(x_1) \psi_j'(x_1) \right) dx_1 + 8I_{55}\frac{1}{\eta^2} \int_0^1 W_l(x_1) \frac{d}{dx_1} \left(U_i'(x_1) \psi_j(x_1) \right) dx_1, \quad (50)$$

$$\begin{aligned}
K_{24}^{NL} = & -12I_{77} \int_0^1 W_l(x_1) \frac{d}{dx_1} \left(W_i'(x_1) W_j'(x_1) W_0'(x_1) \right) dx_1 \\
& + 12I_{00}\eta^2 \int_0^1 W_l(x_1) \frac{d}{dx_1} \left(W_i'(x_1) W_j'(x_1) W_0'^3(x_1) \right) dx_1 \\
& + 12\eta^2 \int_0^1 W_l(x_1) \frac{d}{dx_1} \left(W_i''(x_1) W_j''(x_1) W_0'(x_1) \right) dx_1 \\
& - 24\eta^2 \int_0^1 W_l(x_1) \frac{d^2}{dx_1^2} \left(W_i'(x_1) W_j''(x_1) W_0'(x_1) \right) dx_1, \tag{51}
\end{aligned}$$

$$\begin{aligned}
K_{25}^{NL} = & +24I_{66}\eta \int_0^1 W_l(x_1) \frac{d}{dx_1} \left(W_i''(x_1) \psi_j'(x_1) W_0'(x_1) \right) dx_1 \\
& + 16I_{55} \frac{1}{\eta} \int_0^1 W_l(x_1) \frac{d}{dx_1} \left(W_i'(x_1) \psi_j(x_1) W_0'(x_1) \right) dx_1 \\
& - 24I_{66}\eta \int_0^1 W_l(x_1) \frac{d^2}{dx_1^2} \left(W_i'(x_1) \psi_j'(x_1) W_0'(x_1) \right) dx_1, \tag{52}
\end{aligned}$$

$$\begin{aligned}
K_{26}^{NL} = & +12I_{99} \int_0^1 W_l(x_1) \frac{d}{dx_1} \left(\psi_i'(x_1) \psi_j'(x_1) W_0'(x_1) \right) dx_1 \\
& + 4I_{55} \frac{1}{\eta^2} \int_0^1 W_l(x_1) \frac{d}{dx_1} \left(\psi_i(x_1) \psi_j(x_1) W_0'(x_1) \right) dx_1, \tag{53}
\end{aligned}$$

$$K_{27}^{NL} = +12I_{00} \int_0^1 W_l(x_1) \frac{d}{dx_1} \left(U_i'(x_1) U_j'(x_1) W_k'(x_1) \right) dx_1, \tag{54}$$

$$K_{28}^{NL} = +36I_{00}\eta \int_0^1 W_l(x_1) \frac{d}{dx_1} \left(U_i'(x_1) W_j'(x_1) W_k'(x_1) W_0'(x_1) \right) dx_1, \tag{55}$$

$$\begin{aligned}
K_{29}^{NL} = & -4I_{88} \int_0^1 W_l(x_1) \frac{d}{dx_1} \left(W_i'(x_1) W_j'(x_1) W_k'(x_1) \right) dx_1 \\
& + 24I_{00} \int_0^1 W_l(x_1) \frac{d}{dx_1} \left(W_i'(x_1) W_j'(x_1) W_k'(x_1) W_0'^2(x_1) \right) dx_1 \\
& + 12\eta^2 \int_0^1 W_l(x_1) \frac{d}{dx_1} \left(W_i'(x_1) W_j''(x_1) W_k''(x_1) \right) dx_1 \\
& - 12\eta^2 \int_0^1 W_l(x_1) \frac{d^2}{dx_1^2} \left(W_i'(x_1) W_j'(x_1) W_k''(x_1) \right) dx_1, \tag{56}
\end{aligned}$$

$$\begin{aligned}
K_{210}^{NL} = & +24I_{66}\eta \int_0^1 W_l(x_1) \frac{d}{dx_1} \left(W_i'(x_1) W_j''(x_1) \psi_k'(x_1) \right) dx_1 \\
& +12I_{55} \frac{1}{\eta} \int_0^1 W_l(x_1) \frac{d}{dx_1} \left(W_i'(x_1) W_j'(x_1) \psi_j(x_1) \right) dx_1 \\
& -12I_{66}\eta \int_0^1 W_l(x_1) \frac{d^2}{dx_1^2} \left(W_i'(x_1) W_j'(x_1) \psi_k'(x_1) \right) dx_1,
\end{aligned} \tag{57}$$

$$\begin{aligned}
K_{211}^{NL} = & +12I_{99} \int_0^1 W_l(x_1) \frac{d}{dx_1} \left(W_i'(x_1) \psi_j'(x_1) \psi_k'(x_1) \right) dx_1 \\
& +4I_{55} \frac{1}{\eta^2} \int_0^1 W_l(x_1) \frac{d}{dx_1} \left(W_i'(x_1) \psi_j(x_1) \psi_k(x_1) \right) dx_1,
\end{aligned} \tag{58}$$

$$K_{212}^{NL} = +12I_{00}\eta \int_0^1 W_l(x_1) \frac{d}{dx_1} \left(U_i'(x_1) W_j'(x_1) W_k'(x_1) W_m'(x_1) \right) dx_1, \tag{59}$$

$$K_{213}^{NL} = +15I_{00}\eta^2 \int_0^1 W_l(x_1) \frac{d}{dx_1} \left(W_i'(x_1) W_j'(x_1) W_k'(x_1) W_m'(x_1) W_0'(x_1) \right) dx_1, \tag{60}$$

$$K_{214}^{NL} = +3I_{00}\eta^2 \int_0^1 W_l(x_1) \frac{d}{dx_1} \left(W_i'(x_1) W_j'(x_1) W_k'(x_1) W_m'(x_1) W_n'(x_1) \right) dx_1, \tag{61}$$

$$K_{31}^{NL} = -8I_{55} \int_0^1 \psi_l(x_1) U_i'(x_1) W_j'(x_1) dx_1 + 24I_{66}\eta^2 \int_0^1 \psi_l(x_1) \frac{d}{dx_1} \left(U_j'(x_1) W_j''(x_1) \right) dx_1, \tag{62}$$

$$K_{32}^{NL} = +24I_{99}\eta \int_0^1 \psi_l(x_1) \frac{d}{dx_1} \left(U_i'(x_1) \psi_j'(x_1) \right) dx_1 - 8I_{55} \frac{1}{\eta} \int_0^1 \psi_l(x_1) U_i'(x_1) \psi_j(x_1) dx_1, \tag{63}$$

$$\begin{aligned}
K_{33}^{NL} = & +24I_{66}\eta^3 \int_0^1 \psi_l(x_1) \frac{d}{dx_1} \left(W_i'(x_1) W_j''(x_1) W_0'(x_1) \right) dx_1 \\
& -8I_{55}\eta \int_0^1 \psi_l(x_1) W_i'(x_1) W_j'(x_1) W_0'(x_1) dx_1,
\end{aligned} \tag{64}$$

$$\begin{aligned}
K_{34}^{NL} = & +24I_{99}\eta^2 \int_0^1 \psi_l(x_1) \frac{d}{dx_1} \left(W_i'(x_1) \psi_i'(x_1) W_0'(x_1) \right) dx_1 \\
& -8I_{55} \int_0^1 \psi_l(x_1) W_i'(x_1) \psi_i(x_1) W_0'(x_1) dx_1,
\end{aligned} \tag{65}$$

$$\begin{aligned}
K_{35}^{NL} = & +12I_{66}\eta^3 \int_0^1 \psi_l(x_1) \frac{d}{dx_1} \left(W'_i(x_1) W'_j(x_1) W''_k(x_1) \right) dx_1 \\
& -4I_{55}\eta \int_0^1 \psi_l(x_1) W'_i(x_1) W'_j(x_1) W'_k(x_1) dx_1,
\end{aligned} \tag{66}$$

$$\begin{aligned}
K_{36}^{NL} = & +12I_{99}\eta^2 \int_0^1 \psi_l(x_1) \frac{d}{dx_1} \left(W'_i(x_1) W'_j(x_1) \psi'_k(x_1) \right) dx_1 \\
& -4I_{55} \int_0^1 \psi_l(x_1) W'_i(x_1) W'_j(x_1) \psi_k(x_1) dx_1.
\end{aligned} \tag{67}$$

which by solving the nonlinear polynomial equations of motion using the Newton–Raphson method, the static bending due to the external static force can be obtained.

5 Solution procedure for visco-hyper-elastic vibrations

Using the given nondimensional terms in Sect. 4 and additional nondimensional terms as

$$\Omega = \omega \sqrt{\frac{\rho I_{00} L^4}{C_T I_{44}}}, \quad t^* = t \sqrt{\frac{C_T I_{44}}{\rho A L^4}}, \quad \xi_k = \frac{\xi_k}{C_T} * \sqrt{\frac{C_T I_{44}}{\rho A L^4}}, \tag{68}$$

the nondimensional equations of motion are written as

$$\begin{aligned}
u_{1tt} - \xi_k I_{00} \frac{1}{\eta^2} u_{1x_1 x_1 t} - \xi_k I_{00} \frac{1}{\eta} \frac{\partial}{\partial x_1} (u_{30x_1} u_{3x_1 t}) + 2\xi_k I_{00} \frac{1}{\eta} \frac{\partial}{\partial x_1} (u_{1x_1} u_{1x_1 t}) + 2\xi_k I_{00} \frac{\partial}{\partial x_1} (u_{3x_1} u_{30x_1} u_{1x_1 t}) \\
+ 2\xi_k I_{00} \frac{\partial}{\partial x_1} (u_{1x_1} u_{30x_1} u_{3x_1 t}) - \xi_k I_{77} \frac{1}{\eta} \frac{\partial}{\partial x_1} (u_{3x_1} u_{3x_1 t}) \\
+ 2\xi_k I_{00} \eta \frac{\partial}{\partial x_1} (u_{3x_1} u_{30x_1}^2 u_{3x_1 t}) + 2\xi_k \eta \frac{\partial}{\partial x_1} (u_{3x_1 x_1} u_{3x_1 x_1 t}) \\
+ 2\xi_k I_{66} \frac{\partial}{\partial x_1} (\phi_{x_1} u_{3x_1 x_1 t}) + \xi_k I_{55} \frac{1}{\eta^2} \frac{\partial}{\partial x_1} (\phi u_{3x_1 t}) + 2\xi_k I_{66} \frac{\partial}{\partial x_1} (u_{3x_1 x_1} \phi_{x_1 t}) + \xi_k I_{55} \frac{1}{\eta^2} \frac{\partial}{\partial x_1} (u_{3x_1} \phi_t) \\
+ 2\xi_k I_{99} \frac{1}{\eta} \frac{\partial}{\partial x_1} (\phi_{x_1} \phi_{x_1 t}) + \xi_k I_{55} \frac{1}{\eta^3} \frac{\partial}{\partial x_1} (\phi \phi_t) + \xi_k I_{00} \frac{\partial}{\partial x_1} (u_{3x_1}^2 u_{1x_1 t}) + 2\xi_k I_{00} \frac{\partial}{\partial x_1} (u_{1x_1} u_{3x_1} u_{3x_1 t}) \\
+ 3\xi_k I_{00} \eta \frac{\partial}{\partial x_1} (u_{3x_1}^2 u_{30x_1} u_{3x_1 t}) + \xi_k I_{00} \eta \frac{\partial}{\partial x_1} (u_{3x_1}^3 u_{3x_1 t}) - 8I_{00} \frac{1}{\eta^2} u_{1x_1 x_1} - 8I_{00} \frac{1}{\eta} \frac{\partial}{\partial x_1} (u_{3x_1} u_{30x_1}) \\
+ 12I_{00} \frac{1}{\eta} \frac{\partial}{\partial x_1} (u_{1x_1}^2) + 24I_{00} \frac{\partial}{\partial x_1} (u_{1x_1} u_{3x_1} u_{30x_1}) - 4I_{77} \frac{1}{\eta} \frac{\partial}{\partial x_1} (u_{3x_1}^2) + 12I_{00} \eta \frac{\partial}{\partial x_1} (u_{3x_1}^2 u_{30x_1}^2) \\
+ 12\eta \frac{\partial}{\partial x_1} (u_{3x_1 x_1}^2) + 24I_{66} \frac{\partial}{\partial x_1} (u_{3x_1 x_1} \phi_{x_1}) + 8I_{55} \frac{1}{\eta^2} \frac{\partial}{\partial x_1} (u_{3x_1} \phi) \\
+ 12I_{99} \frac{1}{\eta} \frac{\partial}{\partial x_1} (\phi_{x_1}^2) + 4I_{55} \frac{1}{\eta^3} \frac{\partial}{\partial x_1} (\phi^2) \\
+ 12I_{00} \frac{\partial}{\partial x_1} (u_{1x_1} u_{3x_1}^2) + 12I_{00} \eta \frac{\partial}{\partial x_1} (u_{30x_1} u_{3x_1}^3) + 3I_{00} \eta \frac{\partial}{\partial x_1} (u_{3x_1}^4) = 0,
\end{aligned} \tag{69}$$

$$\begin{aligned}
\frac{I_{66}}{I_{00}} \eta^3 u_{3x_1 t t} + \frac{I_{99}}{I_{00}} \eta^2 \phi_{tt} - \xi_k \eta I_{66} u_{3x_1 x_1 x_1 t} + \frac{1}{2} \xi_k I_{55} \frac{1}{\eta} u_{3x_1 t} - \xi_k I_{99} \phi_{x_1 x_1 t} \\
+ \frac{1}{2} \xi_k I_{55} \frac{1}{\eta^2} \phi_t + 2\xi_k I_{66} \eta^2 \frac{\partial}{\partial x_1} (u_{3x_1 x_1} u_{1x_1 t})
\end{aligned}$$

$$\begin{aligned}
& -\xi_k I_{55} u_{3x_1} u_{1x_1 t} + 2\xi_k I_{99} \eta \frac{\partial}{\partial x_1} (\phi_{x_1} u_{1x_1 t}) - \xi_k I_{55} \frac{1}{\eta} \phi u_{1x_1 t} + 2\xi_k I_{66} \eta^2 \frac{\partial}{\partial x_1} (u_{1x_1} u_{3x_1 x_1 t}) \\
& + 2\xi_k I_{66} \eta^3 \frac{\partial}{\partial x_1} (u_{3x_1 x_1} u_{30x_1} u_{3x_1 t}) - \xi_k I_{55} \eta u_{3x_1} u_{30x_1} u_{3x_1 t} \\
& + \xi_k 2I_{99} \eta^2 \frac{\partial}{\partial x_1} (\phi_{x_1} u_{30x_1} u_{3x_1 t}) - \xi_k I_{55} \phi u_{30x_1} u_{3x_1 t} \\
& + 2\xi_k I_{99} \eta \frac{\partial}{\partial x_1} (u_{1x_1} \phi_{x_1 t}) + 2\xi_k I_{99} \eta^2 \frac{\partial}{\partial x_1} (u_{3x_1} u_{30x_1} \phi_{x_1 t}) + 2\xi_k I_{66} \eta^3 \frac{\partial}{\partial x_1} (u_{3x_1} u_{3x_1 x_1} u_{3x_1 t}) \\
& + \xi_k I_{66} \eta^3 \frac{\partial}{\partial x_1} (u_{3x_1}^2 u_{3x_1 x_1 t}) + 2\xi_k I_{66} \eta^3 \frac{\partial}{\partial x_1} (u_{3x_1} u_{30x_1} u_{3x_1 x_1 t}) \\
& - \xi_k I_{55} \eta u_{3x_1}^2 u_{3x_1 t} + 2\xi_k I_{99} \eta^2 \frac{\partial}{\partial x_1} (u_{3x_1} \phi_{x_1} u_{3x_1 t}) \\
& - \xi_k I_{55} u_{3x_1} \phi u_{3x_1 t} + \xi_k I_{99} \eta^2 \frac{\partial}{\partial x_1} (u_{3x_1}^2 \phi_{x_1 t}) - 8I_{66} \eta u_{3x_1 x_1 x_1} + 8I_{55} \frac{1}{\eta} u_{3x_1} - 8I_{99} \phi_{x_1 x_1} + 8I_{55} \frac{1}{\eta^2} \phi \\
& + 24I_{66} \eta^2 \frac{\partial}{\partial x_1} (u_{1x_1} u_{3x_1 x_1}) - 8I_{55} u_{1x_1} u_{3x_1} + 24I_{99} \eta \frac{\partial}{\partial x_1} (u_{1x_1} \phi_{x_1}) \\
& - 8I_{55} \frac{1}{\eta} u_{1x_1} \phi + 24I_{66} \eta^3 \frac{\partial}{\partial x_1} (u_{3x_1} u_{3x_1 x_1} u_{30x_1}) \\
& - 8I_{55} \eta u_{3x_1}^2 u_{30x_1} + 24I_{99} \eta^2 \frac{\partial}{\partial x_1} (u_{3x_1} \phi_{x_1} u_{30x_1}) - 8I_{55} u_{3x_1} \phi u_{30x_1} \\
& + 12I_{66} \eta^3 \frac{\partial}{\partial x_1} (u_{3x_1}^2 u_{3x_1 x_1}) - 4I_{55} \eta u_{3x_1}^3 \\
& + 12I_{99} \eta^2 \frac{\partial}{\partial x_1} (u_{3x_1}^2 \phi_{x_1}) - 4I_{55} u_{3x_1}^2 \phi = 0.
\end{aligned} \tag{70}$$

$$\begin{aligned}
& -\frac{1}{I_{00}} \eta^2 u_{3x_1 x_1 t t} - \frac{I_{66}}{I_{00}} \eta \phi_{x_1 t t} + u_{3t t} - \xi_k I_{00} \frac{1}{\eta} \frac{\partial}{\partial x_1} (u_{30x_1} u_{1x_1 t}) \\
& + \xi_k u_{3x_1 x_1 x_1 t} - \xi_k I_{00} \frac{\partial}{\partial x_1} (u_{30x_1}^2 u_{3x_1 t}) - \frac{1}{2} \xi_k I_{55} \frac{1}{\eta^2} u_{3x_1 x_1 t} \\
& + \xi_k I_{66} \frac{1}{\eta} \phi_{x_1 x_1 x_1 t} - \frac{1}{2} \xi_k I_{55} \frac{1}{\eta^3} \phi_{x_1 t} + 2\xi_k I_{00} \frac{\partial}{\partial x_1} (u_{1x_1} u_{30x_1} u_{1x_1 t}) \\
& + 2\xi_k I_{00} \eta \frac{\partial}{\partial x_1} (u_{3x_1} u_{30x_1}^2 u_{1x_1 t}) - \xi_k I_{00} \frac{1}{\eta} \frac{\partial}{\partial x_1} (u_{3x_1} u_{1x_1 t}) \\
& - 2\xi_k \eta \frac{\partial^2}{\partial x_1^2} (u_{3x_1 x_1} u_{1x_1 t}) + \xi_k I_{55} \frac{1}{\eta} \frac{\partial}{\partial x_1} (u_{3x_1} u_{1x_1 t}) - 2\xi_k I_{66} \frac{\partial^2}{\partial x_1^2} (\phi_{x_1} u_{1x_1 t}) + \xi_k I_{55} \frac{1}{\eta^2} \frac{\partial}{\partial x_1} (\phi u_{1x_1 t}) \\
& + 2\xi_k I_{00} \eta \frac{\partial}{\partial x_1} (u_{1x_1} u_{30x_1}^2 u_{3x_1 t}) - 2\xi_k \eta \frac{\partial^2}{\partial x_1^2} (u_{1x_1} u_{3x_1 x_1 t}) \\
& - \xi_k I_{77} \frac{\partial}{\partial x_1} (u_{3x_1} u_{30x_1} u_{3x_1 t}) + 2\xi_k I_{00} \eta^2 \frac{\partial}{\partial x_1} (u_{3x_1} u_{30x_1}^3 u_{3x_1 t}) \\
& + 2\xi_k \eta^2 \frac{\partial}{\partial x_1} (u_{3x_1 x_1} u_{30x_1} u_{3x_1 x_1 t}) - \xi_k I_{00} \frac{\partial}{\partial x_1} (u_{30x_1} u_{3x_1} u_{3x_1 t}) \\
& + \xi_k I_{55} \frac{\partial}{\partial x_1} (u_{3x_1} u_{30x_1} u_{3x_1 t}) - 2\xi_k \eta^2 \frac{\partial^2}{\partial x_1^2} (u_{3x_1 x_1} u_{30x_1} u_{3x_1 t}) \\
& + 2\xi_k I_{66} \eta \frac{\partial}{\partial x_1} (\phi_{x_1} u_{30x_1} u_{3x_1 x_1 t}) + 2\xi_k I_{55} \frac{1}{\eta} \frac{\partial}{\partial x_1} (\phi u_{30x_1} u_{3x_1 t}) \\
& - 2\xi_k I_{66} \eta \frac{\partial^2}{\partial x_1^2} (\phi_{x_1} u_{30x_1} u_{3x_1 t}) - 2\xi_k I_{66} \frac{\partial^2}{\partial x_1^2} (u_{1x_1} \phi_{x_1 t})
\end{aligned}$$

$$\begin{aligned}
& +2\xi_k I_{66}\eta \frac{\partial}{\partial x_1} (u_{3x_1x_1} u_{30x_1} \phi_{x_1t}) + \xi_k I_{55} \frac{1}{\eta} \frac{\partial}{\partial x_1} (u_{3x_1} u_{30x_1} \phi_t) \\
& -2\xi_k I_{66}\eta \frac{\partial^2}{\partial x_1^2} (u_{3x_1} u_{30x_1} \phi_{x_1t}) + 2\xi_k I_{99} \frac{\partial}{\partial x_1} (\phi_{x_1} u_{30x_1} \phi_{x_1t}) \\
& +\xi_k I_{55} \frac{1}{\eta^2} \frac{\partial}{\partial x_1} (\phi u_{30x_1} \phi_t) + 2\xi_k I_{00} \frac{\partial}{\partial x_1} (u_{1x_1} u_{3x_1} u_{1x_1t}) \\
& +3\xi_k I_{00}\eta \frac{\partial}{\partial x_1} (u_{3x_1}^2 u_{30x_1} u_{1x_1t}) + 4\xi_k I_{00}\eta \frac{\partial}{\partial x_1} (u_{1x_1} u_{3x_1} u_{30x_1} u_{3x_1t}) \\
& +5\xi_k I_{00}\eta^2 \frac{\partial}{\partial x_1} (u_{3x_1}^2 u_{30x_1}^2 u_{3x_1t}) - \xi_k I_{77} \frac{\partial}{\partial x_1} (u_{3x_1}^2 u_{3x_1t}) \\
& +2\xi_k \eta^2 \frac{\partial}{\partial x_1} (u_{3x_1} u_{3x_1x_1} u_{3x_1x_1t}) - 2\xi_k \eta^2 \frac{\partial^2}{\partial x_1^2} (u_{3x_1} u_{3x_1x_1} u_{3x_1t}) \\
& -\xi_k \eta^2 \frac{\partial^2}{\partial x_1^2} (u_{3x_1}^2 u_{3x_1x_1t}) - 2\xi_k \eta^2 \frac{\partial^2}{\partial x_1^2} (u_{3x_1} u_{30x_1} u_{3x_1x_1t}) \\
& +\xi_k I_{55} \frac{\partial}{\partial x_1} (u_{3x_1}^2 u_{3x_1t}) + 2\xi_k I_{66}\eta \frac{\partial}{\partial x_1} (u_{3x_1} \phi_{x_1} u_{3x_1x_1t}) \\
& +2\xi_k I_{55} \frac{1}{\eta} \frac{\partial}{\partial x_1} (u_{3x_1} \phi u_{3x_1t}) - 2\xi_k I_{66}\eta \frac{\partial^2}{\partial x_1^2} (u_{3x_1} \phi_{x_1} u_{3x_1t}) \\
& +2\xi_k I_{66}\eta \frac{\partial}{\partial x_1} (u_{3x_1} u_{3x_1x_1} \phi_{x_1t}) + \xi_k I_{55} \frac{1}{\eta} \frac{\partial}{\partial x_1} (u_{3x_1}^2 \phi_t) \\
& -\xi_k I_{66}\eta \frac{\partial^2}{\partial x_1^2} (u_{3x_1}^2 \phi_{x_1t}) + 2\xi_k I_{99} \frac{\partial}{\partial x_1} (u_{3x_1} \phi_{x_1} \phi_{x_1t}) + \xi_k I_{55} \frac{1}{\eta^2} \frac{\partial}{\partial x_1} (u_{3x_1} \phi \phi_t) + \xi_k I_{00}\eta \frac{\partial}{\partial x_1} (u_{3x_1}^3 u_{1x_1t}) \\
& +2\xi_k I_{00}\eta \frac{\partial}{\partial x_1} (u_{1x_1} u_{3x_1}^2 u_{3x_1t}) + 4\xi_k I_{00}\eta^2 \frac{\partial}{\partial x_1} (u_{3x_1}^3 u_{30x_1} u_{3x_1t}) \\
& +\xi_k I_{00}\eta^2 \frac{\partial}{\partial x_1} (u_{3x_1}^4 u_{3x_1t}) - 8I_{00} \frac{1}{\eta} \frac{\partial}{\partial x_1} (u_{1x_1} u_{30x_1}) \\
& -8I_{00} \frac{\partial}{\partial x_1} (u_{3x_1} u_{30x_1}^2) + 8u_{3x_1x_1x_1x_1} - 8I_{55} \frac{1}{\eta^2} u_{3x_1x_1} + 8I_{66} \frac{1}{\eta} \phi_{x_1x_1x_1} \\
& -8I_{55} \frac{1}{\eta^3} \phi_{x_1} + 12I_{00} \frac{\partial}{\partial x_1} (u_{1x_1}^2 u_{30x_1}) \\
& -8I_{77} \frac{1}{\eta} \frac{\partial}{\partial x_1} (u_{1x_1} u_{3x_1}) + 24I_{00}\eta \frac{\partial}{\partial x_1} (u_{1x_1} u_{3x_1} u_{30x_1}^2) - 24\eta \frac{\partial^2}{\partial x_1^2} (u_{1x_1} u_{3x_1x_1}) - 24I_{66} \frac{\partial^2}{\partial x_1^2} (u_{1x_1} \phi_{x_1}) \\
& +8I_{55} \frac{1}{\eta^2} \frac{\partial}{\partial x_1} (u_{1x_1} \phi) - 12I_{77} \frac{\partial}{\partial x_1} (u_{3x_1}^2 u_{30x_1}) + 12I_{00}\eta^2 \frac{\partial}{\partial x_1} (u_{3x_1}^2 u_{30x_1}^3) + 12\eta^2 \frac{\partial}{\partial x_1} (u_{3x_1x_1}^2 u_{30x_1}) \\
& -24\eta^2 \frac{\partial^2}{\partial x_1^2} (u_{3x_1} u_{3x_1x_1} u_{30x_1}) + 24I_{66}\eta \frac{\partial}{\partial x_1} (u_{3x_1x_1} \phi_{x_1} u_{30x_1}) + 16I_{55} \frac{1}{\eta} \frac{\partial}{\partial x_1} (u_{3x_1} \phi u_{30x_1}) \\
& -24I_{66}\eta \frac{\partial^2}{\partial x_1^2} (u_{3x_1} \phi_{x_1} u_{30x_1}) + 12I_{99} \frac{\partial}{\partial x_1} (\phi_{x_1}^2 u_{30x_1}) + 4I_{55} \frac{1}{\eta^2} \frac{\partial}{\partial x_1} (\phi^2 u_{30x_1}) + 12I_{00} \frac{\partial}{\partial x_1} (u_{1x_1}^2 u_{3x_1}) \\
& \dots \\
& \dots \\
& +36I_{00}\eta \frac{\partial}{\partial x_1} (u_{1x_1} u_{3x_1}^2 u_{30x_1}) - 4I_{88} \frac{\partial}{\partial x_1} (u_{3x_1}^3) + 24I_{00} \frac{\partial}{\partial x_1} (u_{3x_1}^3 u_{30x_1}^2) + 12\eta^2 \frac{\partial}{\partial x_1} (u_{3x_1} u_{3x_1x_1}^2) \\
& -12\eta^2 \frac{\partial^2}{\partial x_1^2} (u_{3x_1}^2 u_{3x_1x_1}) + 24I_{66}\eta \frac{\partial}{\partial x_1} (u_{3x_1} u_{3x_1x_1} \phi_{x_1}) + 12I_{55} \frac{1}{\eta} \frac{\partial}{\partial x_1} (u_{3x_1}^2 \phi) - 12I_{66}\eta \frac{\partial^2}{\partial x_1^2} (u_{3x_1}^2 \phi_{x_1})
\end{aligned}$$

$$\begin{aligned}
& +12I_{99} \frac{\partial}{\partial x_1} (u_{3x_1} \phi_{x_1}^2) + 4I_{55} \frac{1}{\eta^2} \frac{\partial}{\partial x_1} (u_{3x_1} \phi^2) + 12I_{00} \eta \frac{\partial}{\partial x_1} (u_{1x_1} u_{3x_1}^3) + 15I_{00} \eta^2 \frac{\partial}{\partial x_1} (u_{30x_1} u_{3x_1}^4) \\
& + 3I_{00} \eta^2 \frac{\partial}{\partial x_1} (u_{3x_1}^5) = F \cos(\Omega t), \tag{71}
\end{aligned}$$

For time-dependant analysis, by employing the Galerkin's procedure, the degrees of freedom are written as

$$u_1(x_1, t) = \sum_{j=1}^M U_j(x_1) \mathfrak{R}_j(t), \tag{72}$$

$$u_3(x_1, t) = \sum_{i=1}^N W_i(x_1) \mathfrak{N}_i(t), \tag{73}$$

$$\phi(x_1, t) = \sum_{i=1}^N \psi_i(x_1) \kappa_i(t), \tag{74}$$

and the equations of motion are discretised as

$$\begin{aligned}
& M_{11} \ddot{\mathfrak{R}} + C_{11}^L \dot{\mathfrak{R}} + C_{12}^L \mathfrak{N} + C_{11}^{NL} \mathfrak{R} \dot{\mathfrak{R}} + C_{12}^{NL} \mathfrak{N} \dot{\mathfrak{R}} + C_{13}^{NL} \mathfrak{R} \mathfrak{N} + C_{14}^{NL} \mathfrak{N} \mathfrak{N} + C_{15}^{NL} \kappa \mathfrak{N} + C_{16}^{NL} \mathfrak{N} \kappa + C_{17}^{NL} \kappa \dot{\kappa} \\
& + C_{18}^{NL} \mathfrak{N}^2 \dot{\mathfrak{R}} + C_{19}^{NL} \mathfrak{R} \mathfrak{N} \mathfrak{N} + C_{110}^{NL} \mathfrak{N}^2 \mathfrak{N} + C_{111}^{NL} \mathfrak{N}^3 \mathfrak{N} + K_{11}^L \mathfrak{R} + K_{12}^L \mathfrak{N} + K_{11}^{NL} \mathfrak{R}^2 + K_{12}^{NL} \mathfrak{R} \mathfrak{N} + K_{13}^{NL} \mathfrak{N}^2 \\
& + K_{14}^{NL} \mathfrak{N} \kappa + K_{15}^{NL} \kappa^2 + K_{16}^{NL} \mathfrak{R} \mathfrak{N}^2 + K_{17}^{NL} \mathfrak{N}^3 + K_{18}^{NL} \mathfrak{N}^4 = 0, \tag{75}
\end{aligned}$$

$$\begin{aligned}
& M_{22} \ddot{\mathfrak{N}} + M_{23} \ddot{\kappa} + C_{21}^L \dot{\mathfrak{R}} + C_{22}^L \dot{\mathfrak{N}} + C_{23}^L \dot{\kappa} + C_{21}^{NL} \mathfrak{R} \dot{\mathfrak{R}} + C_{22}^{NL} \mathfrak{N} \dot{\mathfrak{R}} + C_{23}^{NL} \kappa \dot{\mathfrak{R}} + C_{24}^{NL} \mathfrak{R} \dot{\mathfrak{N}} + C_{25}^{NL} \mathfrak{N} \dot{\mathfrak{N}} \\
& + C_{26}^{NL} \kappa \dot{\mathfrak{N}} + C_{27}^{NL} \mathfrak{R} \dot{\kappa} + C_{28}^{NL} \mathfrak{N} \dot{\kappa} + C_{29}^{NL} \kappa \dot{\kappa} + C_{210}^{NL} \mathfrak{R} \mathfrak{N} \dot{\mathfrak{R}} + C_{211}^{NL} \mathfrak{N}^2 \dot{\mathfrak{R}} + C_{212}^{NL} \mathfrak{R} \mathfrak{N} \dot{\mathfrak{N}} + C_{213}^{NL} \mathfrak{N}^2 \dot{\mathfrak{N}} \\
& + C_{214}^{NL} \mathfrak{N} \kappa \dot{\mathfrak{N}} + C_{215}^{NL} \mathfrak{N}^2 \dot{\kappa} + C_{216}^{NL} \mathfrak{N} \kappa \dot{\kappa} + C_{217}^{NL} \mathfrak{N}^3 \dot{\mathfrak{R}} + C_{218}^{NL} \mathfrak{R} \mathfrak{N}^2 \dot{\mathfrak{N}} + C_{219}^{NL} \mathfrak{N}^3 \dot{\mathfrak{N}} + C_{220}^{NL} \mathfrak{N}^4 \dot{\mathfrak{N}} + K_{21}^L \mathfrak{R} \\
& + K_{22}^L \mathfrak{N} + K_{22}^L \kappa + K_{21}^{NL} \mathfrak{R}^2 + K_{22}^{NL} \mathfrak{R} \mathfrak{N} + K_{23}^{NL} \mathfrak{R} \kappa + K_{24}^{NL} \mathfrak{N}^2 \\
& + K_{25}^{NL} \mathfrak{N} \kappa + K_{26}^{NL} \kappa^2 + K_{27}^{NL} \mathfrak{R}^2 \mathfrak{N} + K_{28}^{NL} \mathfrak{R} \mathfrak{N}^2 \\
& + K_{29}^{NL} \mathfrak{N}^3 + K_{210}^{NL} \mathfrak{N}^2 \kappa + K_{211}^{NL} \mathfrak{N} \kappa^2 + K_{212}^{NL} \mathfrak{R} \mathfrak{N}^3 + K_{213}^{NL} \mathfrak{N}^4 + K_{214}^{NL} \mathfrak{N}^5 = F \cos(\Omega t), \tag{76}
\end{aligned}$$

$$\begin{aligned}
& M_{32} \ddot{\mathfrak{N}} + M_{33} \ddot{\kappa} + C_{31}^L \dot{\mathfrak{N}} + C_{32}^L \dot{\kappa} + C_{31}^{NL} \mathfrak{R} \dot{\mathfrak{R}} + C_{32}^{NL} \kappa \dot{\mathfrak{R}} + C_{33}^{NL} \mathfrak{R} \dot{\mathfrak{N}} + C_{34}^{NL} \mathfrak{N} \dot{\mathfrak{N}} + C_{35}^{NL} \kappa \dot{\mathfrak{N}} + C_{36}^{NL} \mathfrak{R} \dot{\kappa} \\
& + C_{37}^{NL} \mathfrak{N} \dot{\kappa} + C_{38}^{NL} \mathfrak{N}^2 \dot{\mathfrak{N}} + C_{39}^{NL} \mathfrak{N} \kappa \dot{\mathfrak{N}} + C_{310}^{NL} \mathfrak{N}^2 \dot{\kappa} + K_{32}^L \mathfrak{N} + K_{33}^L \kappa + K_{31}^{NL} \mathfrak{R} \mathfrak{N} + K_{32}^{NL} \mathfrak{R} \kappa + K_{33}^{NL} \mathfrak{N}^2 \\
& + K_{34}^{NL} \mathfrak{N} \kappa + K_{35}^{NL} \mathfrak{N}^3 + K_{36}^{NL} \mathfrak{N}^2 \kappa = 0, \tag{77}
\end{aligned}$$

with the mass coefficients (M_{ij}) as

$$M_{11} = \int_0^1 U_p(x_1) U_i(x_1) dx_1, \tag{78}$$

$$M_{22} = + \int_0^1 W_l(x_1) W_i(x_1) dx_1 - \frac{1}{I_{00}} \eta^2 \int_0^1 W_l(x_1) W_i''(x_1) dx_1, \tag{79}$$

$$M_{23} = - \frac{I_{66}}{I_{00}} \eta \int_0^1 W_l(x_1) \psi_i'(x_1) dx_1, \tag{80}$$

$$M_{32} = + \frac{I_{66}}{I_{00}} \eta^3 \int_0^1 \psi_l(x_1) W_i'(x_1) dx_1, \tag{81}$$

$$M_{33} = + \frac{I_{99}}{I_{00}} \eta^2 \int_0^1 \psi_l(x_1) \psi_i(x_1) dx_1, \tag{82}$$

and the linear visco-elastic coefficients (C_{ij}^L) as

$$C_{11}^L : -\xi_k I_{00} \frac{1}{\eta^2} \int_0^1 U_l(x_1) U_i''(x_1) dx_1, \quad (83)$$

$$C_{12}^L : -\xi_k I_{00} \frac{1}{\eta} \int_0^1 U_l(x_1) \frac{d}{dx_1} (W_i'(x_1) W_0'(x_1)) dx_1, \quad (84)$$

$$C_{21}^L : -\xi I_{00} \frac{1}{\eta} \int_0^1 W_l(x_1) \frac{d}{dx_1} (U_i'(x_1) W_0'(x_1)) dx, \quad (85)$$

$$C_{22}^L : +\xi \int_0^1 W_l(x_1) W_i^{(4)}(x_1) dx_1 - \xi I_{00} \int_0^1 W_l(x_1) \frac{d}{dx_1} (W_i'(x_1) W_0^2(x_1)) dx_1 - \frac{1}{2} \xi I_{55} \frac{1}{\eta^2} \int_0^1 W_l(x_1) W_i''(x_1) dx_1, \quad (86)$$

$$C_{23}^L : +\xi I_{66} \frac{1}{\eta} \int_0^1 W_l(x_1) \psi_i'''(x_1) dx_1 - \frac{1}{2} \xi I_{55} \frac{1}{\eta^3} \int_0^1 W_l(x_1) \psi_i'(x_1) dx_1, \quad (87)$$

$$C_{31}^L : -\xi_k \eta I_{66} \int_0^1 \psi_l(x_1) W_i'''(x_1) dx_1 + \frac{1}{2} \xi_k I_{55} \frac{1}{\eta} \int_0^1 \psi_l(x_1) W_i'(x_1) dx_1, \quad (88)$$

$$C_{32}^L : -\xi_k I_{99} \int_0^1 \psi_l(x_1) \psi_i''(x_1) dx_1 + \frac{1}{2} \xi_k I_{55} \frac{1}{\eta^2} \int_0^1 \psi_l(x_1) \psi_i(x_1) dx_1. \quad (89)$$

The nonlinear damping coefficients (C_{ij}^{NL}) are shown in Appendix C for the sake of brevity, and the stiffness terms are defined in the previous sections. By solving the dynamic equilibrium equations [39,41], the nonlinear vibration response of the system is obtained.

6 Results and discussions for bending and vibration

In this section, the nonlinear bending and vibration responses of thick visco-hyper-elastic shallow arches are modelled for different cases of curvature, slenderness ratio and internal resonances. The hyper-elastic properties are taken from Ref [55] for vulcanised rubbers with the Mooney–Rivlin coefficients as $C_1 = 0.28e6$ Pa and $C_2 = 0.15e6$ Pa and mass density $\rho = 950$ kg/m³.

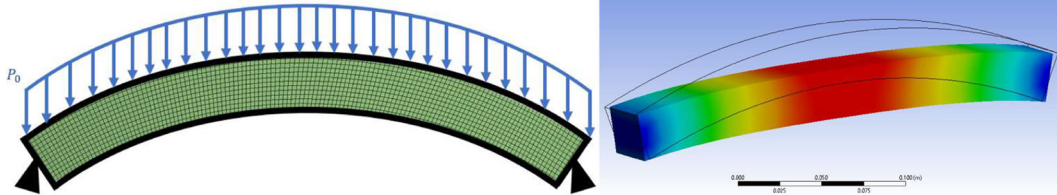
6.1 Bending analysis

Study 1: Force-bending analysis

As the first part of the analysis, the nonlinear static deformation of thick hyper-elastic shallow arches is analysed following the solution procedure given in Sect. 4 and compared to those obtained using finite element software. The shallow arch is assumed to have the following geometrical properties: $L = 0.3$ m, $h = 0.03$ m, $b = 0.03$ m, with a simply supported boundary condition and assumed to undergo a static pressure (which is varied from -1 to 1 kPa). The maximum transverse deformation is obtained and shown in Table 1 for different curvatures and external loads. By comparing the current results with those obtained from ANSYS [56], it is shown that the results are in very good agreement. Besides, it can be seen that by increasing the curvature term, the maximum deformation of the shallow arch decreases significantly especially for higher external loadings.

Table 1 Comparison of the maximum transverse deformation of the shallow arch for different loads

$R_0 = u_{30}/h$	Maximum transverse deformation (mm)						
	P_0	-1 kPa	-500 Pa	-200 Pa	200 Pa	500 Pa	1 kPa
0.5	Present	6.1184	3.5272	1.6645	2.0481	5.9868	12.2926
	ANSYS	6.4259	3.6742	1.6301	1.9701	6.1897	12.7670
1.0	Present	2.9103	1.5246	0.6643	0.6984	1.7256	3.6963
	ANSYS	3.0089	1.5804	0.6533	0.6861	1.7877	3.8807
1.5	Present	1.7133	0.8725	0.3582	0.3607	0.9051	1.8352
	ANSYS	1.7517	0.8930	0.3616	0.3678	0.9320	1.9089



Moreover, to understand the static behaviour of the shallow arch under different types of loadings, the curvature is assumed as following the first mode as $W_0(x_1) = R_0 W_1(x_1)$ where R_0 is the nondimensional curvature term assumed as 0.6. The nondimensional external applied static force (F_{bending}) is modelled using a combination of sin functions as

$$F_{\text{bending}}(x) : f_1 \sin(\pi x) + f_2 \sin(2\pi x), \quad f_1 = 50(n-1), \quad f_2 = 25(n-1), \quad (90)$$

where n is varied from 1 to 70. For the given function, the static force through the length of the arch is shown in Fig. 3a for different values of n . By solving the nonlinear bending equilibrium equations, the nondimensional deformations of the hyper-elastic thick arch are shown in Fig. 3b–d. It can be seen that there is a high coupling between the degrees of freedom; also, the force type and magnitude can change the deformations in the structure, significantly.

Study 2: Influence of the curvature on the bending behaviour

For the same shallow arch with the given properties in the previous subsection, the influence of the curvature in resisting deformation in the structure is analysed. To do this, an external static force following Eq. (93) is given to the structure with f_1 and f_2 as 1000 and -500 , respectively. Figure 4a–c shows the axial, transverse and rotation deformation of the shallow arch by varying the curvature term as $R_0 = 0.1, 0.3, 0.5, 0.7, 0.9, 1.0$, and 1.5 . It can be seen that increasing the shallow arch curvature leads to higher resistance against the transverse loading. Besides, as shown in Fig. 4a, the coupling between the axial and transverse deformations increases significantly by increasing the curvature term.

Study 3: Influence of considering the higher-order nonlinear terms

Since incompressible hyper-elastic structures show nonlinearity in their constitutive equation as well as large deformations, the importance of considering the higher-order nonlinear terms is discussed in this subsection. Accordingly, for the same shallow arch in previous sections with the curvature of $R_0 = 1.5$, bending behaviour is obtained using both linear and nonlinear models when subjected to an external static force following Eq. (93) with f_1 and f_2 as 10000 and -2500 . Figure 5a–c shows the axial, transverse and rotation deformation of the shallow arch by only considering the linear part of the equilibrium equations as well as considering the full equations. It can be seen that the linear simplification of the structure leads to underestimated bending deformations for the axial deformation and inaccurate transverse and rotation motions which indicates the importance of accurately modelling the nonlinear behaviour of the structure.

6.2 Internal resonance and vibration analysis

Study 1: Vibration in the hyper-elasticity framework with internal resonances

Since the curvature of the thick, soft shallow arch can change the linear frequencies of the structure, this section concentrates on detecting the internal resonance behaviour of the arch due to the curvature. For the same shallow arch model given in Sect. 6.1, the ratio of the second natural frequency to the fundamental

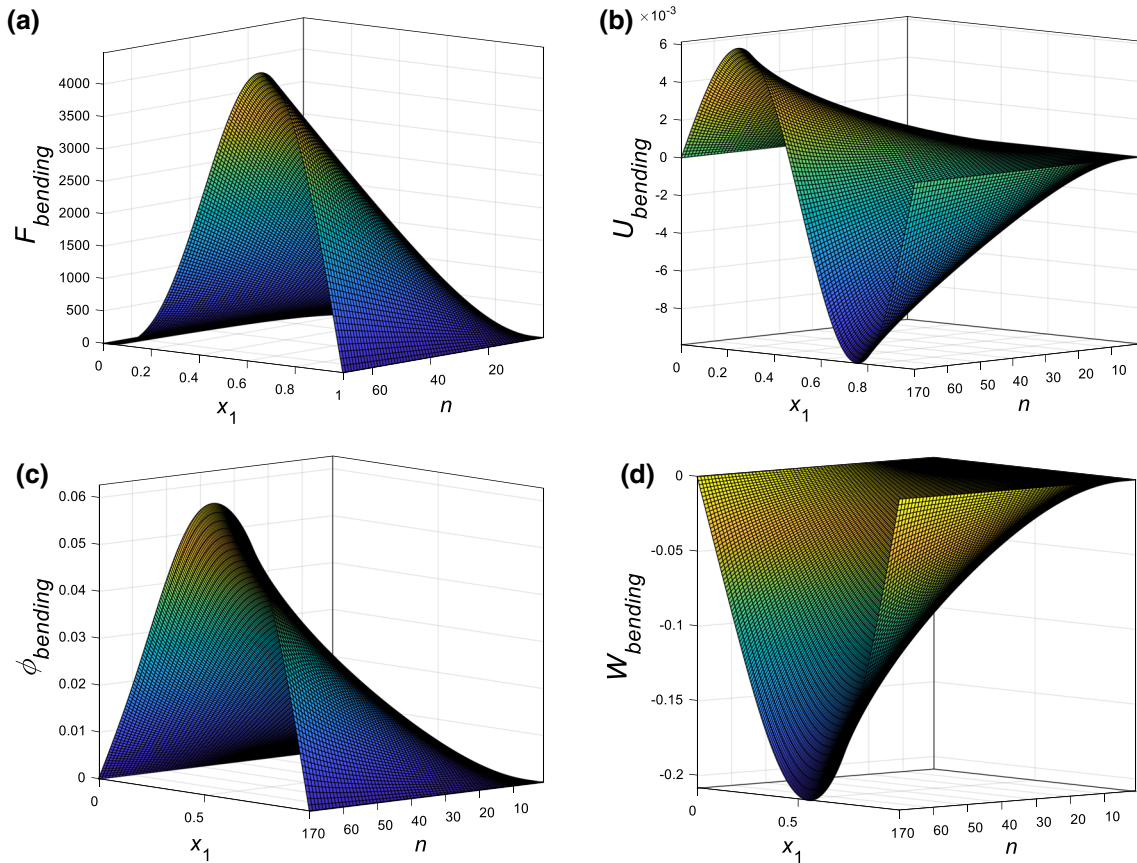


Fig. 3 Nondimensional static force and nondimensional bending deformation response of the hyper-elastic arch **a** applied force, **b** axial deformation, **c** transverse deformation and **d** rotational deformation

natural frequency (ω_2/ω_1) is shown in Fig. 6 by having different curvature terms. It can be seen that around $R_0 = 0.3$, the ratio is equal to 3 and the three-to-one internal resonance in the system occurs. Accordingly, by having $R_0 = 0.3$ (which leads to $\omega_2/\omega_1 \cong 3$), the frequency-amplitude responses of the system are shown in Figs. 7, 8 and 9 for the dominant vibration coordinates in the axial, transverse and rotational directions. It can be seen that a high coupling between modes is obtained, and the system shows a rich nonlinear behaviour, with a combination of hardening, softening and modal interactions.

Study 2: Vibration in the visco-hyper-elasticity framework with internal resonances

Many soft structures show visco-elastic behaviour together with hyper-elasticity (especially biological tissues). To see the influence of this combination on the nonlinear frequency response of the structure with an internal resonance, this section analyses the visco-hyper-elasticity behaviour of thick, soft, shallow arches. Since visco-elasticity is a function of many environmental parameters, such as temperature [57], this property of hyper-elastic structures should be measured for specific working environments. In this study, visco-elasticity is modelled using the Kelvin–Voigt visco-hyper-elastic model which has been shown that has a good accuracy in modelling visco-hyper-elastic materials [48]. The influence of the visco-elasticity on the three-to-one internal resonance of the structure is shown in Figs. 10, 11 and 12 for the axial, transverse and rotational directions by varying the viscoelastic parameter as $\xi_k = [2e-3, 2e-4, 2e-5]$. It can be seen that the visco-hyper-elasticity has a significant effect in changing the nonlinear frequency response, and increasing this term from $2e-5$ to $2e-4$ decreases the maximum amplitude. By increasing the viscous term to $2e-3$, the complicated nonlinear internal resonance behaviour will be fully damped.

Study 3: Curvature sensitivity

One of the main concentrations of this paper is on considering the curvature modelling in soft thick shallow arches. To show the importance and influence of this term on the nonlinear vibration behaviour of the structure, the shallow arch is assumed to have the following geometrical properties given in Sect. 6.1 with a simply supported boundary condition and curvature term varied as $R_0 = [0.0, 0.1, 0.3, 0.5, 0.6, 0.8, 1.0]$.

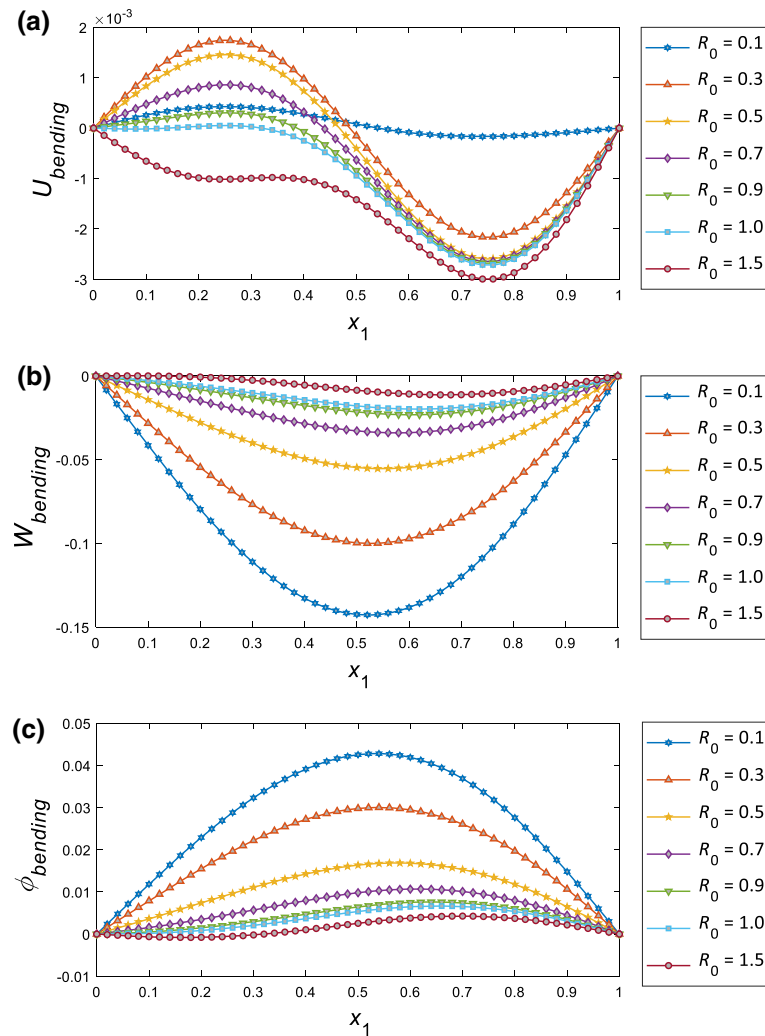


Fig. 4 The nondimensional bending deformation response of the hyper-elastic shallow arch with different curvatures **a** axial deformation, **b** transverse deformation and **c** rotational deformation

The results for the amplitude-frequency response of the soft arch subjected to an external nondimensional load of $F = 0.5$ are shown in Figs. 13, 14 and 15 for the dominant vibration coordinates in the axial, transverse and rotation directions, respectively. It can be seen that increasing the curvature term from 0 to 1.0 moves the amplitude responses to higher frequencies. For higher curvature terms, transverse dynamic equilibriums show a softening effect, while for lower curvature term a combination of hardening and softening behaviour is obtained. Furthermore, by increasing the curvature term, the maximum amplitude of the first transverse dynamic equilibrium coordinate decreases significantly.

Study 4: Slenderness ratio sensitivity

Since a third-order shear deformable model has been used, different length-to-thickness models can be analysed. In this subsection, by assuming the same properties given in Sect. 6.1, the length of the arch is varied to $L = S_L h$ where S_L is the slenderness ratio, which is varied as $S_L = [10, 20, 30, 40, 50]$. The results for varying the length-to-thickness ratio are shown in Figs. 16, 17 and 18 for the axial, transverse and rotation dynamic equilibrium directions. It can be seen that increasing the slenderness ratio increases the stiffness hardening behaviour in the transverse coordinates. The first axial and rotation coordinates' amplitude decreases by increasing the slenderness ratio rate, which means the coupling between the axial and the transverse motion decreases and the rotation motion loses its importance.

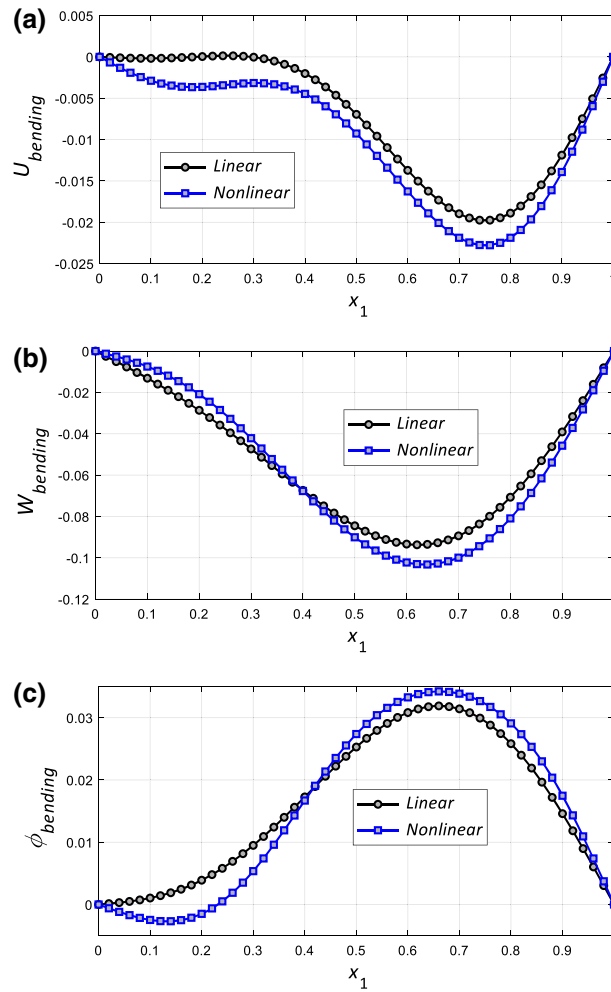


Fig. 5 Comparison of the linear and nonlinear models for bending analysis of the hyper-elastic shallow arch with $R_0 = 1.5$ **a** axial deformation, **b** transverse deformation, and **c** rotational deformation

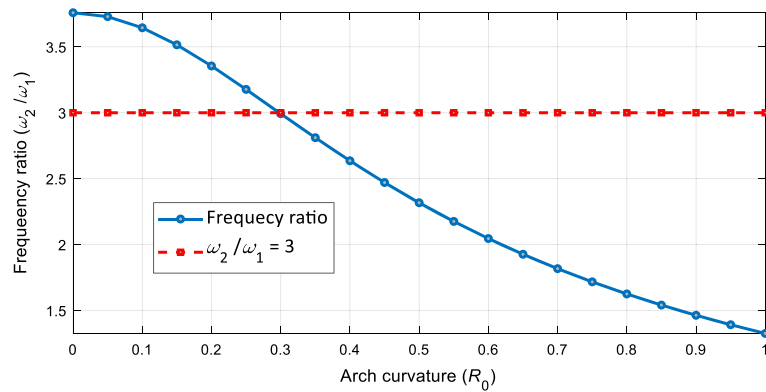


Fig. 6 The frequency ratio of a soft, thick shallow arch with respect to the curvature term

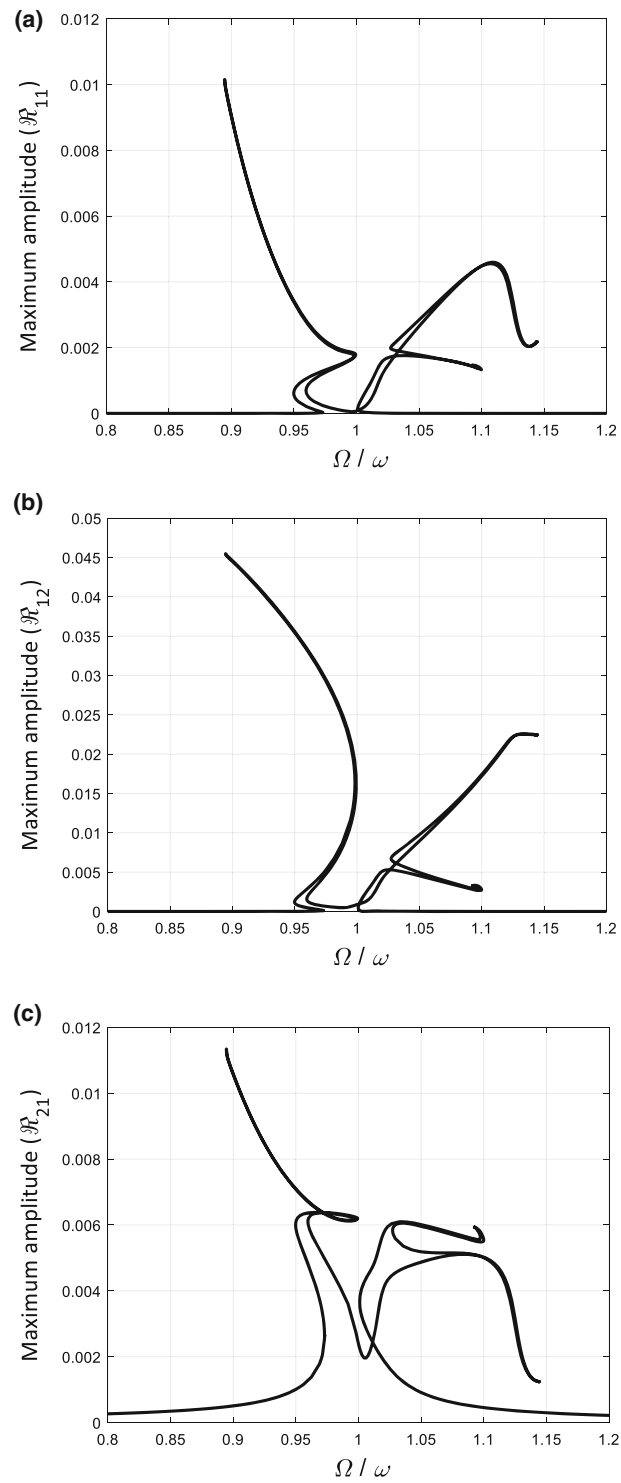


Fig. 7 First three axial nonlinear frequency responses of *hyper-elastic* thick, soft arches at the internal resonance **a** \mathfrak{R}_{11} , **b** \mathfrak{R}_{21} and **c** \mathfrak{R}_{12}

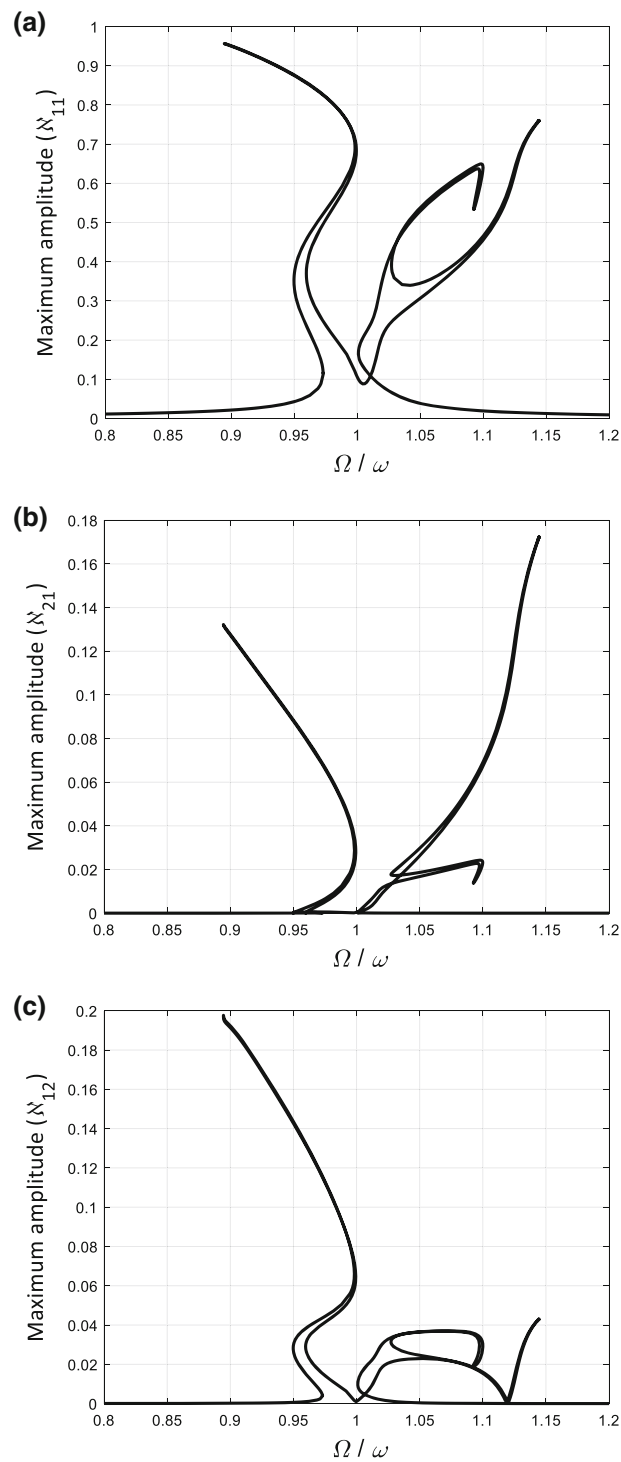


Fig. 8 First three *transverse* nonlinear frequency responses of *hyper-elastic* thick, soft arches at the *internal resonance* **a** N_{11} , **b** N_{12} and **c** N_{21}

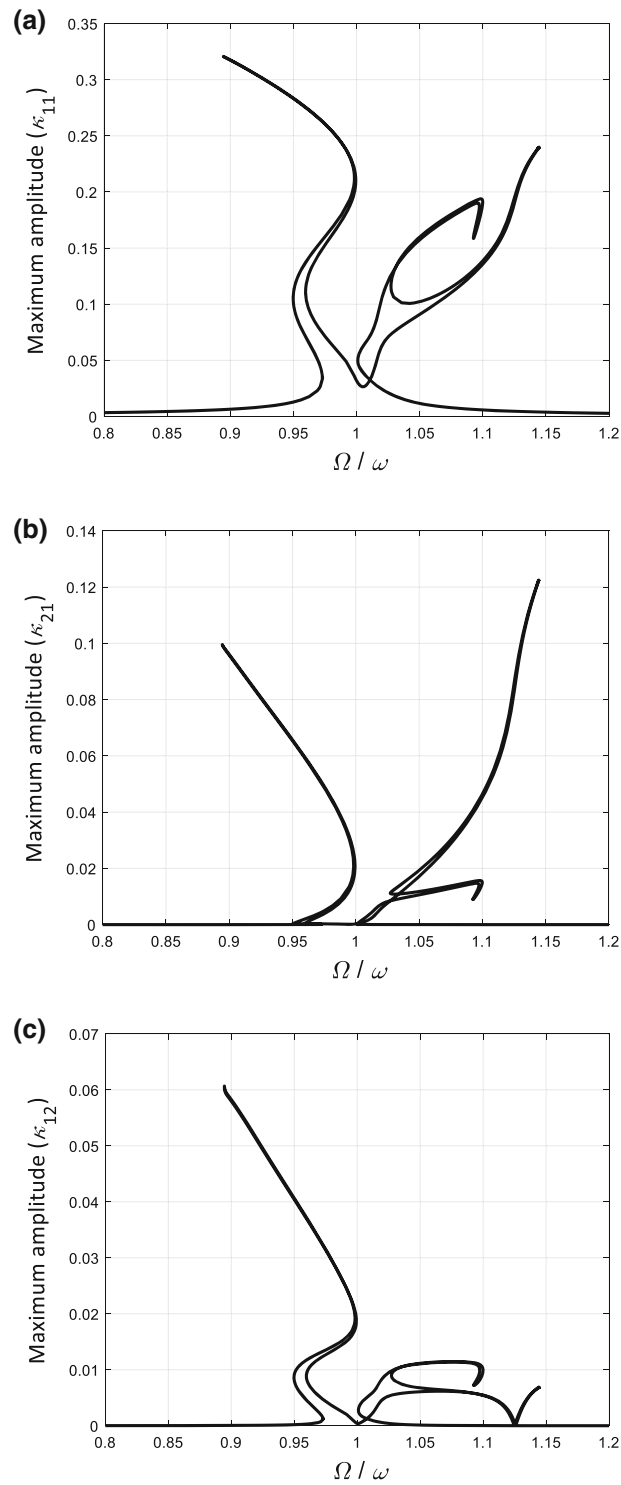


Fig. 9 First three *rotation* nonlinear frequency responses of *hyper-elastic* thick, soft arches at the *internal resonance* **a** κ_{11} , **b** κ_{21} and **c** κ_{12}

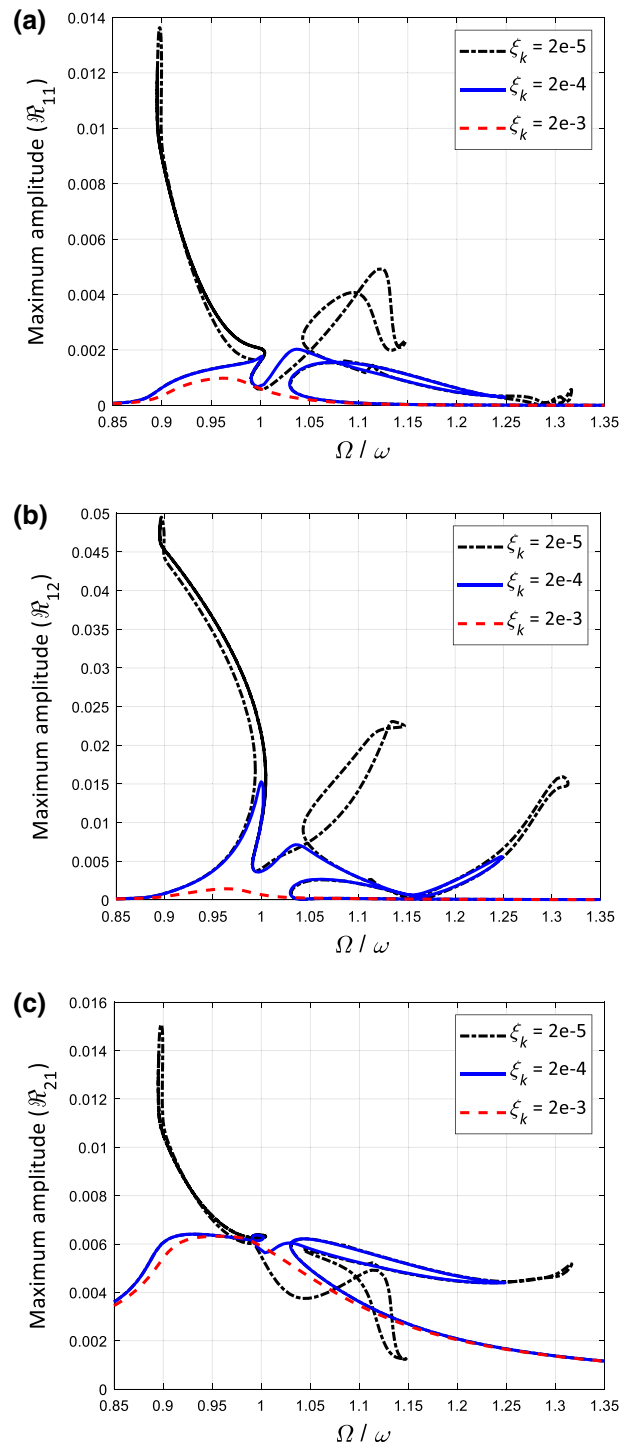


Fig. 10 First three *axial* nonlinear frequency responses of visco-hyper-elastic thick, soft arches at the internal resonance **a** \mathfrak{R}_{11} , **b** \mathfrak{R}_{21} and **c** \mathfrak{R}_{12}

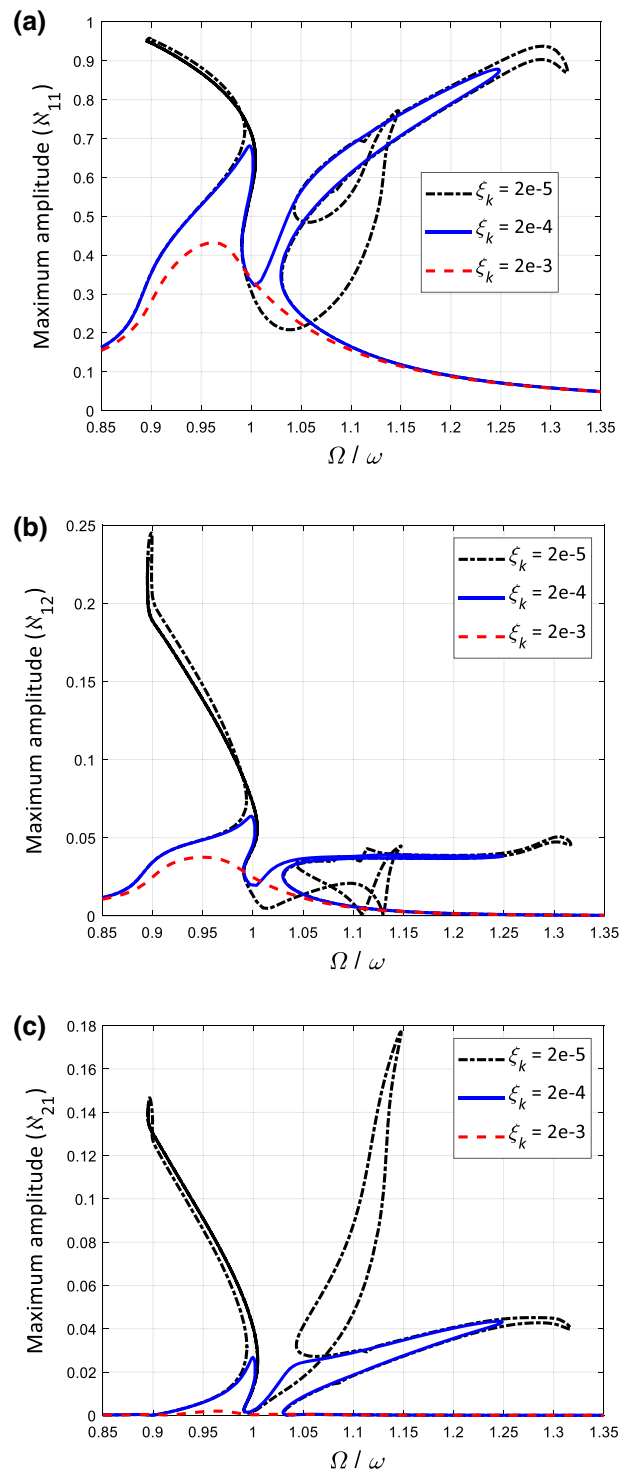


Fig. 11 First three *transverse* nonlinear frequency responses of *visco-hyper-elastic* thick, soft arches at the *internal resonance* **a** N_{11} , **b** N_{12} and **c** N_{21}

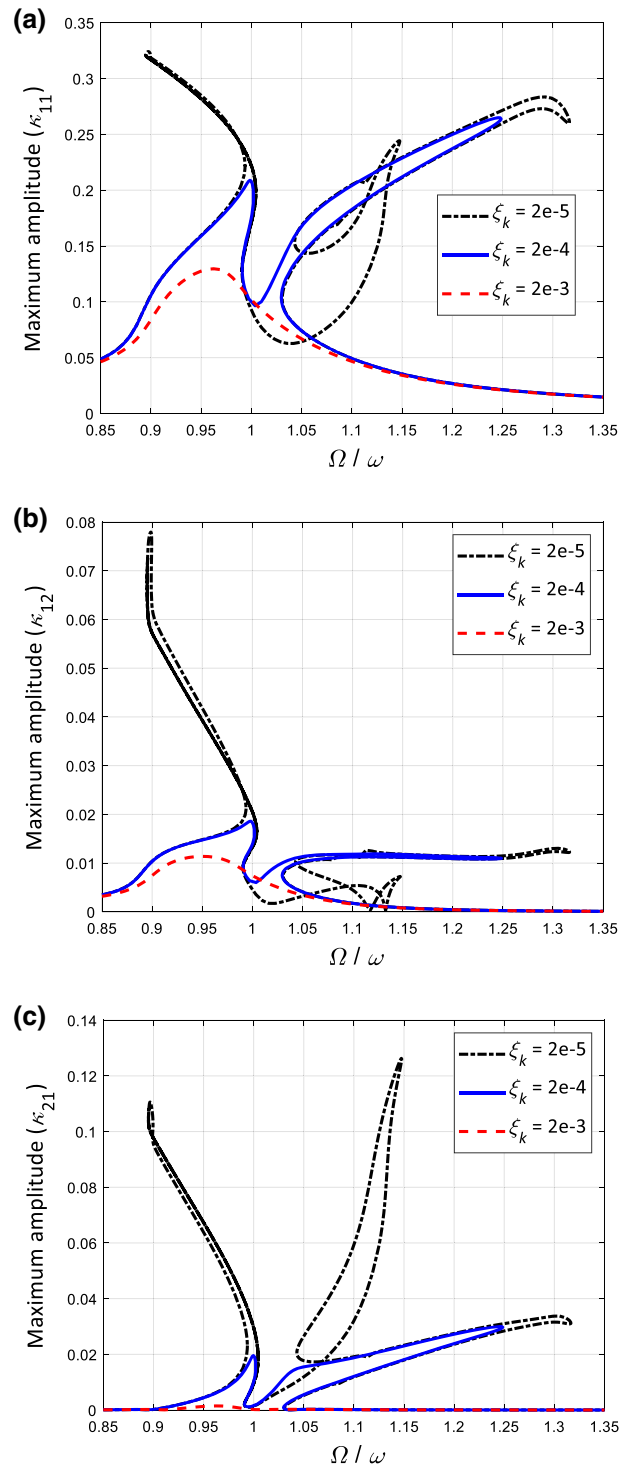


Fig. 12 First three rotation nonlinear frequency responses of visco-hyper-elastic thick, soft arches at the internal resonance **a** κ_{11} , **b** κ_{21} and **c** κ_{12}

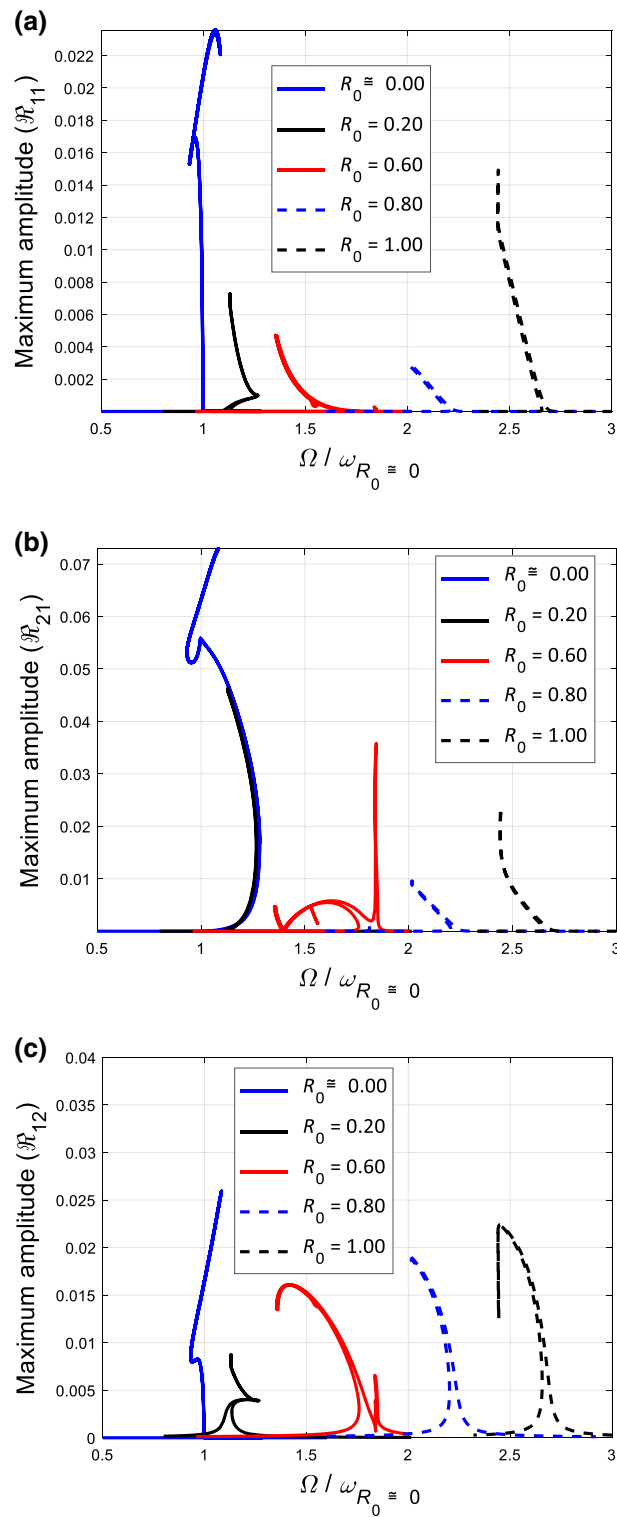


Fig. 13 Influence of the *curvature term* on the first three *axial* nonlinear frequency responses of thick, soft arches **a** \mathfrak{R}_{11} , **b** \mathfrak{R}_{21} and **c** \mathfrak{R}_{12}

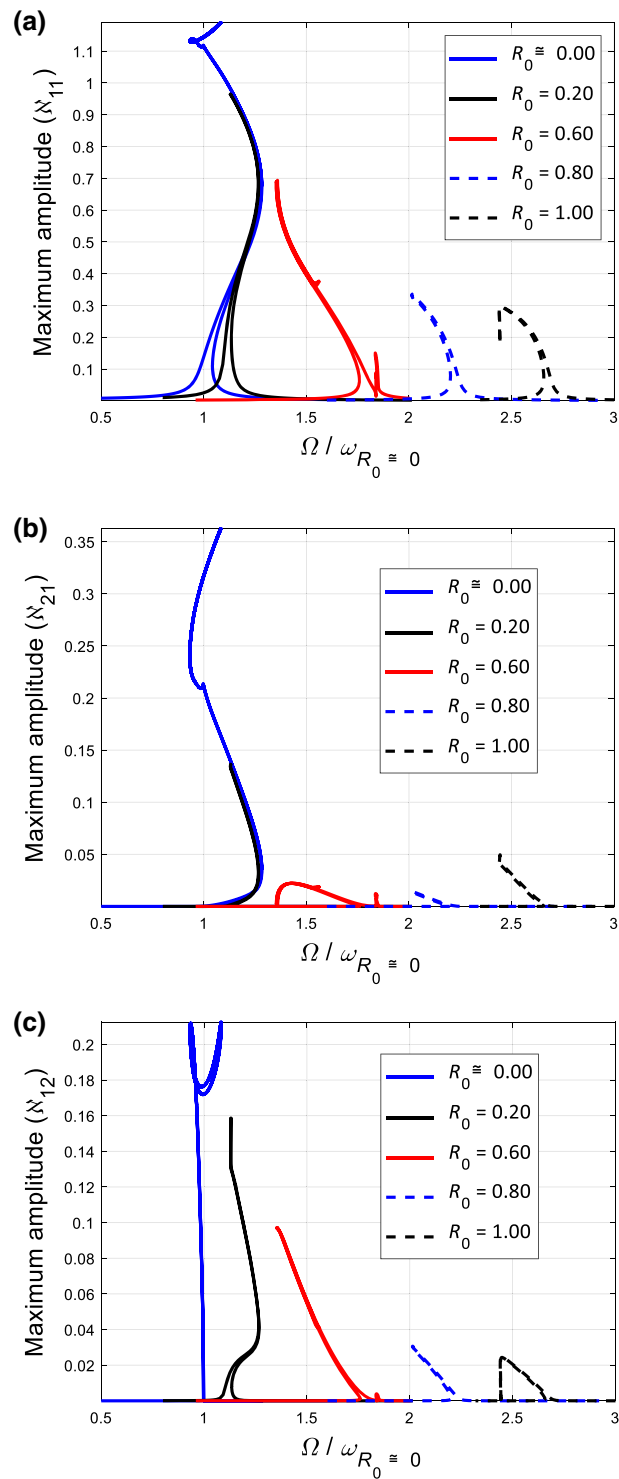


Fig. 14 Influence of the curvature term on the first three transverse nonlinear frequency responses of thick, soft arches **a** \mathcal{N}_{11} , **b** \mathcal{N}_{12} and **(c)** \mathcal{N}_{21}

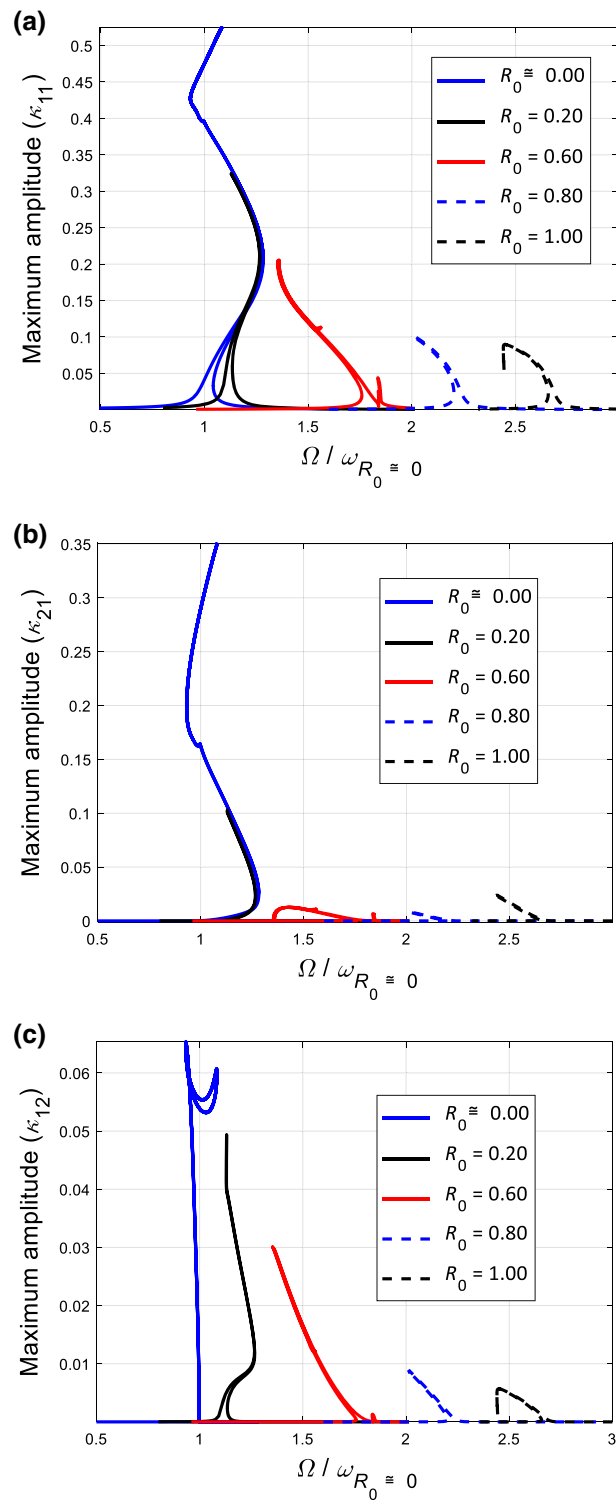


Fig. 15 Influence of the *curvature term* on the first three *rotation nonlinear frequency responses* of thick, soft arches **a** κ_{11} , **b** κ_{21} and **c** κ_{12}

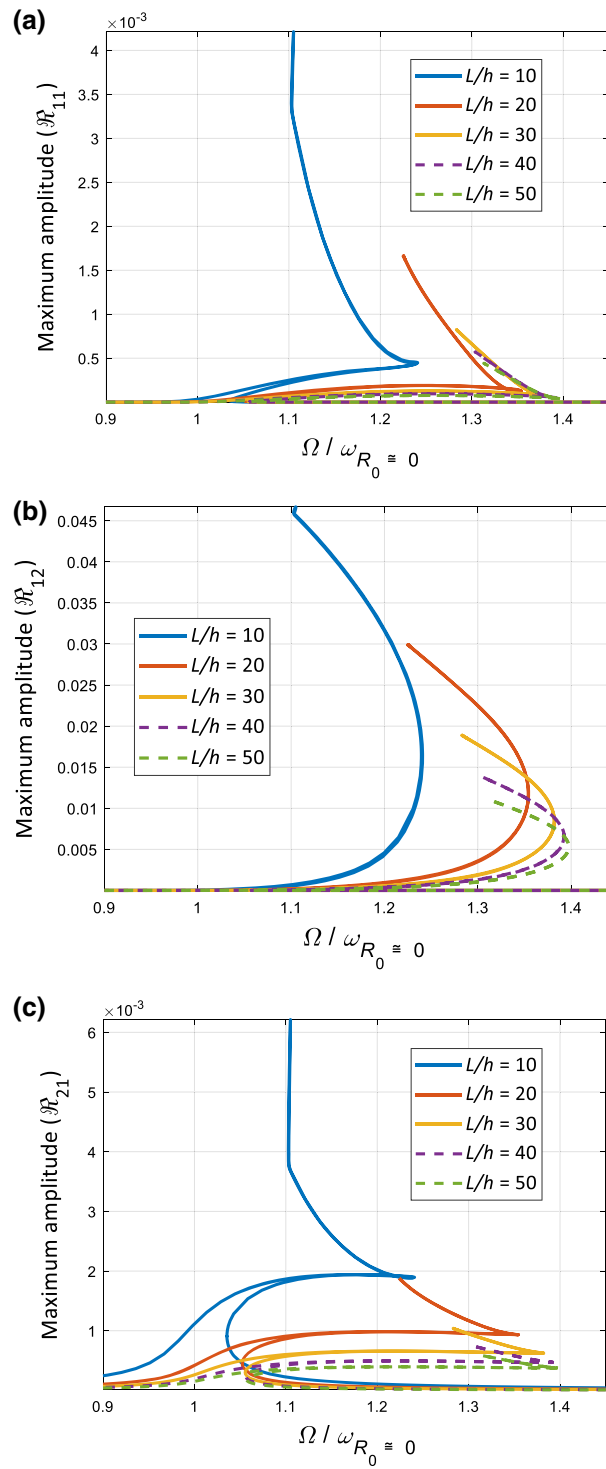


Fig. 16 Influence of the *slenderness ratio* on the first three *axial* nonlinear frequency responses of thick, soft arches **a** \mathfrak{R}_{11} , **b** \mathfrak{R}_{21} and **c** \mathfrak{R}_{12}

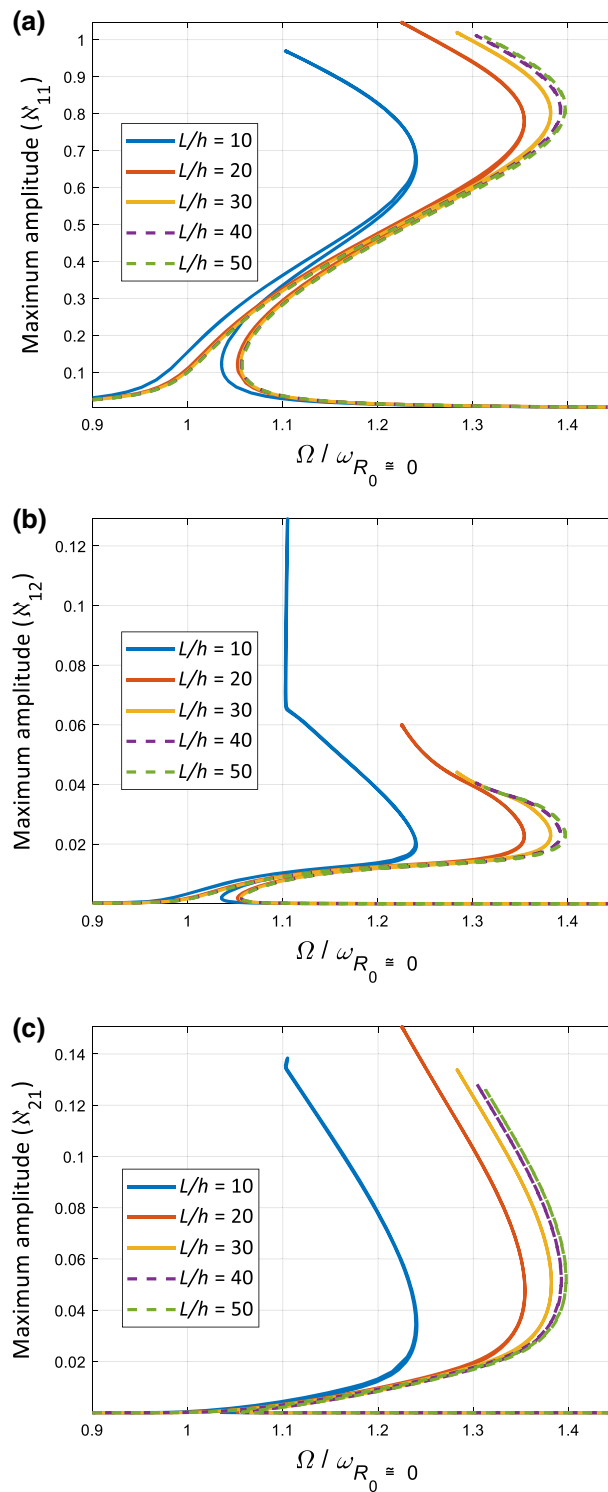


Fig. 17 Influence of the *slenderness ratio* on the first three *transverse* nonlinear frequency responses of thick, soft arches **a** \mathcal{N}_{11} , **b** \mathcal{N}_{12} and **c** \mathcal{N}_{21}

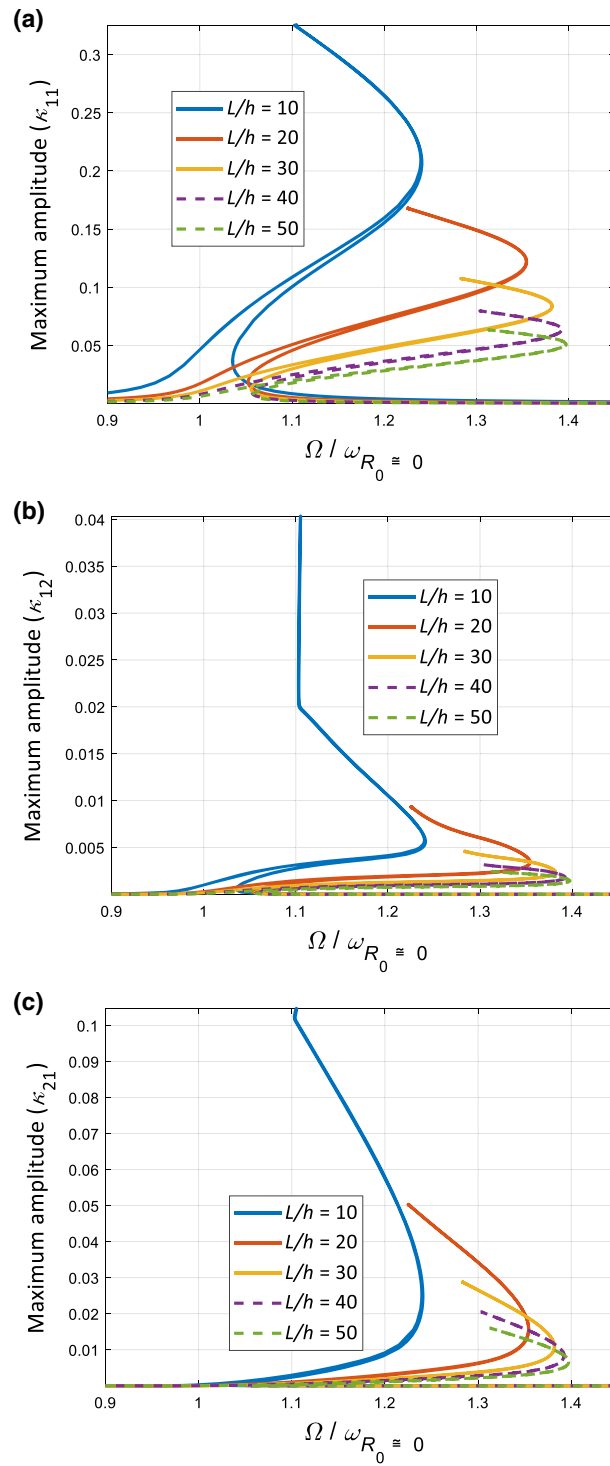


Fig. 18 Influence of the *slenderness ratio* on the first three *transverse nonlinear frequency responses* of thick, soft arches **a** κ_{11} , **b** κ_{12} and **c** κ_{21}

7 Summary and conclusions

The nonlinear bending and vibration behaviours of simply supported, thick, soft, visco-hyper-elastic shallow arches are examined in this study. The visco-hyper-elasticity was modelled using an incompressible Mooney–Rivlin’s hyper-elastic strain energy density model, together with Kelvin–Voigt visco-hyper-elasticity. A higher-order shear deformable model was used to model the axial, transverse and rotation motions. The curvature term was added to the model using von Kármán geometric nonlinearity, and the incompressibility condition was satisfied in the strain–displacement definition. The coupled nonlinear equations of motion were obtained and solved using force-moment balance method and the virtual work method for the vibration and bending analyses, respectively, showing that:

- (i) Increasing the shallow arch curvature leads to higher resistance against the transverse loading in all axial, transverse and rotation motions of the structure and changed the bending behaviour significantly.
- (ii) The linear simplification of the structure leads to underestimated bending deformations for all the axial, transverse and rotation motions which indicates the importance of accurately modelling the nonlinear behaviour of the structure.
- (iii) The coupling between the axial and transverse bending increases significantly by increasing the curvature term
- (iv) The curvature term can cause internal resonance in the system, leading to high coupling between modes, for which the system shows a rich nonlinear behaviour with a combination of hardening, softening and modal interactions.
- (v) The visco-hyper-elasticity has a significant effect in changing the nonlinear frequency response with a three-to-one internal resonance. By increasing the visco-hyper-elastic term to higher numbers, the complicated nonlinear internal resonance behaviour will be fully damped.
- (vi) For higher curvature terms, transverse dynamic equilibriums show a softening behaviour, while for lower curvature terms, a combination of hardening and softening behaviour is obtained.
- (vii) By increasing the curvature term, the maximum amplitude of the first transverse dynamic equilibrium coordinate decreases significantly.
- (viii) Increasing the slenderness ratio increases the stiffness hardening behaviour in the transverse coordinates.
- (ix) The dominant axial and rotation coordinates’ amplitude decreases by increasing the slenderness ratio rate, which means the coupling between the axial and the transverse motion decreases and the rotation motion loses its importance.

Acknowledgements This work employed the supercomputing resources provided by the Phoenix HPC service at the University of Adelaide. The HDR scholarship support through The University of Adelaide and Faculty of Engineering, Computer & Mathematical Sciences, The University of Adelaide is also acknowledged.

Open Access This article is licensed under a Creative Commons Attribution 4.0 International License, which permits use, sharing, adaptation, distribution and reproduction in any medium or format, as long as you give appropriate credit to the original author(s) and the source, provide a link to the Creative Commons licence, and indicate if changes were made. The images or other third party material in this article are included in the article’s Creative Commons licence, unless indicated otherwise in a credit line to the material. If material is not included in the article’s Creative Commons licence and your intended use is not permitted by statutory regulation or exceeds the permitted use, you will need to obtain permission directly from the copyright holder. To view a copy of this licence, visit <http://creativecommons.org/licenses/by/4.0/>.

Funding Open Access funding enabled and organized by CAUL and its Member Institutions Open Access funding enabled and organized by CAUL and its Member Institutions. No funding was received for this project.

Declarations

Conflict of interest The authors declare that they have no known competing financial interests or personal relationships that could have appeared to influence the work reported in this paper.

Appendix A

Variations of potential energy terms

$$PE1 = -8C_T I_{00} u_{1x_1 x_1} - 8C_T I_{00} \frac{d}{dx_1} (u_{3x_1} u_{30x_1}) - 8C_T I_{22} u_{3x_1 x_1 x_1} - 8C_T I_{33} \phi_{x_1 x_1} + 12C_T I_{00} \frac{d}{dx_1} (u_{1x_1}^2)$$

$$\begin{aligned}
& +24C_T I_{00} \frac{d}{dx_1} (u_{1x_1} u_{3x_1} u_{30x_1}) + 24C_T I_{22} \frac{d}{dx_1} (u_{1x} u_{3x_1 x_1}) \\
& +24C_T I_{33} \frac{d}{dx_1} (u_{1x_1} \phi_{x_1}) - 4C_T I_{77} \frac{d}{dx_1} (u_{3x_1}^2) \\
& +12C_T I_{00} \frac{d}{dx_1} (u_{3x_1}^2 u_{30x_1}^2) + 24C_T I_{22} \frac{d}{dx_1} (u_{3x_1} u_{3x_1 x_1} u_{03x_1}) + 12C_T I_{44} \frac{d}{dx_1} (u_{3x_1 x_1}^2) \\
& +24C_T I_{33} \frac{d}{dx_1} (u_{3x_1} \phi_{x_1} u_{30x_1}) + 24C_T I_{66} \frac{d}{dx_1} (u_{3x_1 x_1} \phi_{x_1}) \\
& +8C_T I_{55} \frac{d}{dx_1} (u_{3x_1} \phi) + 12C_T I_{99} \frac{d}{dx_1} (\phi_{x_1}^2) \\
& +4C_T I_{55} \frac{d}{dx_1} (\phi^2) + 12C_T I_{00} \frac{d}{dx_1} (u_{1x_1} u_{3x_1}^2) + 12C_T I_{00} \frac{d}{dx_1} (u_{30} u_{3x_1}^3) + 12C_T I_{22} \frac{d}{dx_1} (u_{3x_1}^2 u_{3x_1 x_1}) \\
& +12C_T I_{33} \frac{d}{dx_1} (u_{3x_1}^2 \phi_{x_1}) + 3C_T I_{00} \frac{\partial}{\partial x_1} (u_{3x_1}^4), \tag{A.1}
\end{aligned}$$

$$\begin{aligned}
PE3 = & -8C_T I_{33} u_{1x_1 x_1} - 8C_T I_{33} \frac{d}{dx_1} (u_{3x_1} u_{30x_1}) - 8C_T I_{66} u_{3x_1 x_1 x_1} \\
& +8C_T I_{55} u_{3x_1} - 8C_T I_{99} \phi_{x_1 x_1} + 8C_T I_{55} \phi \\
& +12C_T I_{33} \frac{d}{dx_1} (u_{1x_1}^2) + 24C_T I_{33} \frac{d}{dx_1} (u_{1x_1} u_{3x_1} u_{30x_1}) + 24C_T I_{66} \frac{d}{dx_1} (u_{1x_1} u_{3x_1 x_1}) - 8C_T I_{55} u_{1x_1} u_{3x_1} \\
& +24C_T I_{99} \frac{d}{dx_1} (u_{1x_1} \phi_{x_1}) - 8C_T I_{55} u_{1x_1} \phi - 4C_T I_{33} \frac{d}{dx_1} (u_{3x_1}^2) + 12C_T I_{33} \frac{d}{dx_1} (u_{3x_1}^2 u_{30x_1}^2) \\
& +24C_T I_{66} \frac{d}{dx_1} (u_{3x_1} u_{3x_1 x_1} u_{30x_1}) + 4C_T I_{1313} \frac{d}{dx_1} (u_{3x_1}^2) + 12C_T I_{1414} \frac{d}{dx_1} (u_{3x_1 x_1}^2) - 8C_T I_{55} u_{3x_1}^2 u_{30x_1} \\
& -8C_T I_{1111} u_{3x_1} u_{3x_1 x_1} + 24C_T I_{99} \frac{d}{dx_1} (u_{3x_1} \phi_{x_1} u_{30x_1}) \\
& +24C_T I_{1515} \frac{d}{dx_1} (u_{3x_1 x_1} \phi_{x_1}) + 8C_T I_{1313} \frac{d}{dx_1} (u_{3x_1} \phi) \\
& -8C_T I_{1313} u_{3x_1} \phi_{x_1} - 8C_T I_{55} u_{3x_1} \phi u_{30x_1} - 8C_T I_{1111} u_{3x_1 x_1} \phi \\
& +12C_T I_{1616} \frac{d}{dx_1} (\phi_{x_1}^2) + 4C_T I_{1313} \frac{d}{dx_1} (\phi^2) \\
& -8C_T I_{1313} \phi \phi_{x_1} + 12C_T I_{33} \frac{d}{dx_1} (u_{1x_1} u_{3x_1}^2) \\
& +12C_T I_{33} \frac{d}{dx_1} (u_{30x_1} u_{3x_1}^3) + 12C_T I_{66} \frac{d}{dx_1} (u_{3x_1}^2 u_{3x_1 x_1}) \\
& -4C_T I_{55} u_{3x_1}^3 + 12C_T I_{99} \frac{d}{dx_1} (u_{3x_1}^2 \phi_{x_1}) - 4C_T I_{55} u_{3x_1}^2 \phi + 3C_T I_{33} \frac{d}{dx_1} (u_{3x_1}^4), \tag{A.2}
\end{aligned}$$

$$\begin{aligned}
PE2 = & +8C_T I_{22} u_{1x_1 x_1 x_1} - 8C_T I_{00} \frac{d}{dx_1} (u_{1x_1} u_{30x_1}) - 8C_T I_{00} \frac{d}{dx_1} (u_{3x_1} u_{30x_1}^2) - 8C_T I_{22} \frac{d}{dx_1} (u_{30x_1} u_{3x_1 x_1}) \\
& +8C_T I_{22} \frac{d^2}{dx_1^2} (u_{3x_1} u_{30x_1}) + 8C_T I_{44} u_{3x_1 x_1 x_1 x_1} - 8C_T I_{55} u_{3x_1 x_1} \\
& +8C_T I_{66} \phi_{x_1 x_1 x_1} - 8C_T I_{33} \frac{d}{dx_1} (\phi_{x_1} u_{30x_1}) \\
& -8C_T I_{55} \phi_{x_1} - 12C_T I_{22} \frac{d^2}{dx_1^2} (u_{1x_1}^2) + 12C_T I_{00} \frac{d}{dx_1} (u_{1x_1}^2 u_{30x_1}) - 8C_T I_{77} \frac{d}{dx_1} (u_{1x_1} u_{3x_1}) \\
& +24C_T I_{00} \frac{d}{dx_1} (u_{1x_1} u_{3x_1} u_{30x_1}^2) - 24C_T I_{22} \frac{d^2}{dx_1^2} (u_{1x_1} u_{3x_1} u_{30x_1}) + 24C_T I_{22} \frac{d}{dx_1} (u_{1x_1} u_{3x_1 x_1} u_{30x_1}) \\
& -24C_T I_{44} \frac{d^2}{dx_1^2} (u_{1x_1} u_{3x_1 x_1}) + 24C_T I_{33} \frac{d}{dx_1} (u_{1x_1} \phi_{x_1} u_{30x_1}) - 24C_T I_{66} \frac{d^2}{dx_1^2} (u_{1x_1} \phi_{x_1})
\end{aligned}$$

$$\begin{aligned}
& +4C_T I_{22} \frac{d^2}{dx_1^2} (u_{3x_1}^2) - 4C_T I_{1111} \frac{d^2}{dx_1^2} (u_{3x_1}^2) - 12C_T I_{1010} \frac{d^2}{dx_1^2} (u_{3x_1x_1}^2) - 12C_T I_{77} \frac{d}{dx_1} (u_{3x_1}^2 u_{30x_1}) \\
& - 8C_T I_{1212} \frac{d}{dx_1} (u_{3x_1} u_{3x_1x_1}) + 12C_T I_{00} \frac{d}{dx_1} (u_{3x_1}^2 u_{30x_1}^3) + 12C_T I_{44} \frac{d}{dx_1} (u_{3x_1x_1}^2 u_{30x_1}) \\
& + 24C_T I_{22} \frac{d}{dx_1} (u_{3x_1} u_{3x_1x_1} u_{30x_1}^2) - 12C_T I_{22} \frac{d^2}{dx_1^2} (u_{3x_1}^2 u_{30x_1}^2) - 24C_T I_{44} \frac{d^2}{dx_1^2} (u_{3x_1} u_{3x_1x_1} u_{30x_1}) \\
& - 8C_T I_{33} \frac{d}{dx_1} (u_{30x_1} \phi_{x_1}) + 8C_T I_{1313} \frac{d}{dx_1} (u_{3x_1} \phi_{x_1}) + 24C_T I_{33} \frac{d}{dx_1} (u_{3x_1} \phi_{x_1} u_{30x_1}^2) \\
& + 24C_T I_{66} \frac{d}{dx_1} (u_{3x_1x_1} \phi_{x_1} u_{30x_1}) + 16C_T I_{55} \frac{d}{dx_1} (u_{3x_1} \phi u_{30x_1}) - 8C_T I_{1111} \frac{d^2}{dx_1^2} (u_{3x_1} \phi) \\
& - 24C_T I_{66} \frac{d^2}{dx_1^2} (u_{3x_1} \phi_{x_1} u_{30x_1}) - 24C_T I_{1414} \frac{d^2}{dx_1^2} (u_{3x_1x_1} \phi_{x_1}) + 8C_T I_{1111} \frac{d}{dx_1} (u_{3x_1x_1} \phi) \\
& - 4C_T I_{1111} \frac{d^2}{dx_1^2} (\phi^2) - 12C_T I_{1515} \frac{d^2}{dx_1^2} (\phi_{x_1}^2) + 12C_T I_{99} \frac{d}{dx_1} (\phi_{x_1}^2 u_{30x_1}) + 8C_T I_{55} \frac{d}{dx_1} (u_{1x_1} \phi) \\
& + 4C_T I_{55} \frac{d}{dx_1} (\phi^2 u_{30x_1}) + 8C_T I_{1313} \frac{d}{dx_1} (\phi \phi_{x_1}) + 12C_T I_{00} \frac{d}{dx_1} (u_{1x_1}^2 u_{3x_1}) \\
& + 36C_T I_{00} \frac{d}{dx_1} (u_{1x_1} u_{3x_1}^2 u_{30x_1}) + 24C_T I_{22} \frac{d}{dx_1} (u_{1x_1} u_{3x_1} u_{3x_1x_1}) - 12C_T I_{22} \frac{d^2}{dx_1^2} (u_{1x_1} u_{3x_1}^2) \\
& + 24C_T I_{33} \frac{d}{dx_1} (u_{1x_1} u_{3x_1} \phi_{x_1}) - 4C_T I_{88} \frac{d}{dx_1} (u_{3x_1}^3) + 24C_T I_{00} \frac{d}{dx_1} (u_{3x_1}^3 u_{30x_1}^2) \\
& - 12C_T I_{22} \frac{d^2}{dx_1^2} (u_{30x_1} u_{3x_1}^3) + 12C_T I_{44} \frac{d}{dx_1} (u_{3x_1} u_{3x_1x_1}^2) + 36C_T I_{22} \frac{d}{dx_1} (u_{3x_1}^2 u_{3x_1x_1} u_{30x_1}) \\
& - 12C_T I_{44} \frac{d^2}{dx_1^2} (u_{3x_1}^2 u_{3x_1x_1}) + 36C_T I_{33} \frac{d}{dx_1} (u_{3x_1}^2 \phi_{x_1} u_{30x_1}) + 24C_T I_{66} \frac{d}{dx_1} (u_{3x_1} u_{3x_1x_1} \phi_{x_1}) \\
& + 12C_T I_{55} \frac{d}{dx_1} (u_{3x_1}^2 \phi) - 12C_T I_{66} \frac{d^2}{dx_1^2} (u_{3x_1}^2 \phi_x) + 12C_T I_{99} \frac{d}{dx_1} (u_{3x_1} \phi_{x_1}^2) \\
& + 4C_T I_{55} \frac{d}{dx_1} (u_{3x_1} \phi^2) + 12C_T I_{00} \frac{d}{dx_1} (u_{1x_1} u_{3x_1}^3) - 3C_T I_{22} \frac{d^2}{dx_1^2} (u_{3x_1}^4) \\
& + 15C_T I_{00} \frac{d}{dx_1} (u_{30x_1} u_{3x_1}^4) + 12C_T I_{22} \frac{d}{dx_1} (u_{3x_1}^3 u_{3x_1x_1}) \\
& + 12C_T I_{33} \frac{d}{dx_1} (u_{3x_1}^3 \phi_{x_1}) + 3C_T I_{00} \frac{d}{dx_1} (u_{3x_1}^5), \tag{A.3}
\end{aligned}$$

Appendix B

For homogeneous visco-hyper-elastic shallow arches, due to the homogeneity of the visco-hyper-elastic arch, some of the inertia terms are equal to zero, simplifying the equations of motion to

$$\begin{aligned}
& \rho I_{00} u_{1tt} - \xi_k I_{00} u_{1x_1x_1t} - \xi_k I_{00} \frac{\partial}{\partial x_1} (u_{30x_1} u_{3x_1t}) + 2\xi_k I_{00} \frac{\partial}{\partial x_1} (u_{1x_1} u_{1x_1t}) + 2\xi_k I_{00} \frac{\partial}{\partial x_1} (u_{3x_1} u_{30x_1} u_{x_1t}) \\
& + 2\xi_k I_{00} \frac{\partial}{\partial x_1} (u_{1x_1} u_{30x_1} u_{3x_1t}) - \xi_k I_{77} \frac{\partial}{\partial x_1} (u_{3x_1} u_{3x_1t}) + 2\xi_k I_{00} \frac{\partial}{\partial x_1} (u_{3x_1} u_{30x_1}^2 u_{3x_1t}) - 8C_T I_{00} u_{1x_1x_1} \\
& + 2\xi_k I_{44} \frac{\partial}{\partial x_1} (u_{3x_1x_1} u_{3x_1x_1t}) + 2\xi_k I_{66} \frac{\partial}{\partial x_1} (\phi_{x_1} u_{3x_1x_1t}) + \xi_k I_{55} \frac{\partial}{\partial x_1} (\phi u_{3x_1t}) + 2\xi_k I_{66} \frac{\partial}{\partial x_1} (u_{3x_1x_1} \phi_{x_1t}) \\
& + \xi_k I_{55} \frac{\partial}{\partial x_1} (u_{3x_1} \phi_t) + 2\xi_k I_{99} \frac{\partial}{\partial x_1} (\phi_{x_1} \phi_{x_1t}) + \xi_k I_{55} \frac{\partial}{\partial x_1} (\phi \phi_t) + \xi_k I_{00} \frac{\partial}{\partial x_1} (u_{3x_1}^2 u_{xt}) + \xi_k I_{00} \frac{\partial}{\partial x_1} (u_{3x_1}^3 u_{3x_1t})
\end{aligned}$$

$$\begin{aligned}
& +2\xi_k I_{00} \frac{\partial}{\partial x_1} (u_{1x_1} u_{3x_1} u_{3x_1 t}) + 3\xi_k I_{00} \frac{\partial}{\partial x_1} (u_{3x_1}^2 u_{30x_1} u_{3x_1 t}) - 8C_T I_{00} \frac{\partial}{\partial x_1} (u_{3x_1} u_{30x_1}) + 12C_T I_{00} \frac{\partial}{\partial x_1} (u_{1x_1}^2) \\
& +24C_T I_{00} \frac{\partial}{\partial x_1} (u_{1x_1} u_{3x_1} u_{30x_1}) - 4C_T I_{77} \frac{\partial}{\partial x_1} (u_{3x_1}^2) + 12C_T I_{00} \frac{\partial}{\partial x_1} (u_{3x_1}^2 u_{30x_1}^2) + 12C_T I_{44} \frac{\partial}{\partial x_1} (u_{3x_1}^2 u_{3x_1 t}) \\
& +24C_T I_{66} \frac{\partial}{\partial x_1} (u_{3x_1} \phi_{x_1}) + 8C_T I_{55} \frac{\partial}{\partial x_1} (u_{3x_1} \phi) + 12C_T I_{99} \frac{\partial}{\partial x_1} (\phi_{x_1}^2) + 4C_T I_{55} \frac{\partial}{\partial x_1} (\phi^2) \\
& +12C_T I_{00} \frac{\partial}{\partial x_1} (u_{1x_1} u_{3x_1}^2) + 12C_T I_{00} \frac{\partial}{\partial x_1} (u_{30x_1} u_{3x_1}^3) + 3C_T I_{00} \frac{\partial}{\partial x_1} (u_{3x_1}^4) = 0, \tag{B.1}
\end{aligned}$$

$$\begin{aligned}
& -\rho I_{44} u_{3x_1 x_1 t t} - \rho I_{66} \phi_{x_1 t t} + \rho I_{00} u_{3t t} - \xi_k I_{00} \frac{\partial}{\partial x_1} (u_{30x_1} u_{1x_1 t}) + \xi_k I_{44} u_{3x_1 x_1 x_1 t} - \xi_k I_{00} \frac{\partial}{\partial x_1} (u_{30x_1}^2 u_{3x_1 t}) \\
& -\frac{1}{2} \xi_k I_{55} u_{3x_1 x_1 t} + \xi_k I_{66} \phi_{x_1 x_1 t} - \frac{1}{2} \xi_k I_{55} \phi_{x_1 t} + 2\xi_k I_{00} \frac{\partial}{\partial x_1} (u_{1x_1} u_{30x_1} u_{1x_1 t}) + 2\xi_k I_{00} \frac{\partial}{\partial x_1} (u_{3x_1} u_{30x_1}^2 u_{1x_1 t}) \\
& -\xi_k I_{00} \frac{\partial}{\partial x_1} (u_{3x_1} u_{1x_1 t}) - 2\xi_k I_{44} \frac{\partial^2}{\partial x_1^2} (u_{3x_1 x_1} u_{1x_1 t}) + \xi_k I_{55} \frac{\partial}{\partial x_1} (u_{3x_1} u_{1x_1 t}) - 2\xi_k I_{66} \frac{\partial^2}{\partial x_1^2} (\phi_{x_1} u_{1x_1 t}) \\
& +\xi_k I_{55} \frac{\partial}{\partial x_1} (\phi u_{1x_1 t}) + 2\xi_k I_{00} \frac{\partial}{\partial x_1} (u_{1x_1} u_{30x_1}^2 u_{3x_1 t}) - 2\xi_k I_{44} \frac{\partial^2}{\partial x_1^2} (u_{1x_1} u_{3x_1 x_1 t}) - \xi_k I_{77} \frac{\partial}{\partial x_1} (u_{3x_1} u_{30x_1} u_{3x_1 t}) \\
& +2\xi_k I_{00} \frac{\partial}{\partial x_1} (u_{3x_1} u_{30x_1}^3 u_{3x_1 t}) + 2\xi_k I_{44} \frac{\partial}{\partial x_1} (u_{3x_1 x_1} u_{30x_1} u_{3x_1 x_1 t}) - \xi_k I_{00} \frac{\partial}{\partial x_1} (u_{30x_1} u_{3x_1} u_{3x_1 t}) \\
& +\xi_k I_{55} \frac{\partial}{\partial x_1} (u_{3x_1} u_{30x_1} u_{3x_1 t}) - 2\xi_k I_{44} \frac{\partial^2}{\partial x_1^2} (u_{3x_1 x_1} u_{30x_1} u_{3x_1 t}) + 2\xi_k I_{66} \frac{\partial}{\partial x_1} (\phi_{x_1} u_{30x_1} u_{3x_1 x_1 t}) \\
& +2\xi_k I_{55} \frac{\partial}{\partial x_1} (\phi u_{30x_1} u_{3x_1 t}) - 2\xi_k I_{66} \frac{\partial^2}{\partial x_1^2} (\phi_{x_1} u_{30x_1} u_{3x_1 t}) \\
& -2\xi_k I_{66} \frac{\partial^2}{\partial x_1^2} (u_{1x_1} \phi_{x_1 t}) + 2\xi_k I_{66} \frac{\partial}{\partial x_1} (u_{3x_1 x_1} u_{30x_1} \phi_{x_1 t}) \\
& +\xi_k I_{55} \frac{\partial}{\partial x_1} (u_{3x_1} u_{30x_1} \phi_t) - 2\xi_k I_{66} \frac{\partial^2}{\partial x_1^2} (u_{3x_1} u_{30x_1} \phi_{x_1 t}) \\
& +2\xi_k I_{99} \frac{\partial}{\partial x_1} (\phi_{x_1} u_{30x_1} \phi_{x_1 t}) + \xi_k I_{55} \frac{\partial}{\partial x_1} (\phi u_{30x_1} \phi_t) \\
& +2\xi_k I_{00} \frac{\partial}{\partial x_1} (u_x u_{3x_1} u_{1x_1 t}) + 3\xi_k I_{00} \frac{\partial}{\partial x_1} (u_{3x_1}^2 u_{30x_1} u_{1x_1 t}) + 4\xi_k I_{00} \frac{\partial}{\partial x_1} (u_{1x_1} u_{3x_1} u_{30x_1} u_{3x_1 t}) \\
& +5\xi_k I_{00} \frac{\partial}{\partial x_1} (u_{3x_1}^2 u_{30x_1}^2 u_{3x_1 t}) - \xi_k I_{77} \frac{\partial}{\partial x_1} (u_{3x_1}^2 u_{3x_1 t}) + 2\xi_k I_{44} \frac{\partial}{\partial x_1} (u_{3x_1} u_{3x_1 x_1} u_{3x_1 x_1 t}) \\
& \dots \\
& \dots \\
& -2\xi_k I_{44} \frac{\partial^2}{\partial x_1^2} (u_{3x_1} u_{3x_1 x_1} u_{3x_1 t}) - \xi_k I_{44} \frac{\partial^2}{\partial x_1^2} (u_{3x_1}^2 u_{3x_1 x_1 t}) \\
& -2\xi_k I_{44} \frac{\partial^2}{\partial x_1^2} (u_{3x_1} u_{30x_1} u_{3x_1 x_1 t}) + \xi_k I_{55} \frac{\partial}{\partial x_1} (u_{3x_1}^2 u_{3x_1 t}) \\
& +2\xi_k I_{66} \frac{\partial}{\partial x_1} (u_{3x_1} \phi_{x_1} u_{3x_1 x_1 t}) + 2\xi_k I_{55} \frac{\partial}{\partial x_1} (u_{3x_1} \phi u_{3x_1 t}) \\
& -2\xi_k I_{66} \frac{\partial^2}{\partial x_1^2} (u_{3x_1} \phi_{x_1} u_{3x_1 t}) + 2\xi_k I_{66} \frac{\partial}{\partial x_1} (u_{3x_1} u_{3x_1 x_1} \phi_{x_1 t}) \\
& +\xi_k I_{55} \frac{\partial}{\partial x_1} (u_{3x_1}^2 \phi_t) - \xi_k I_{66} \frac{\partial^2}{\partial x_1^2} (u_{3x_1}^2 \phi_{x_1 t}) + 2\xi_k I_{99} \frac{\partial}{\partial x_1} (u_{3x_1} \phi_{x_1} \phi_{x_1 t}) + \xi_k I_{55} \frac{\partial}{\partial x_1} (u_{3x_1} \phi \phi_t) \\
& +\xi_k I_{00} \frac{\partial}{\partial x_1} (u_{3x_1}^3 u_{1x_1 t}) + 2\xi_k I_{00} \frac{\partial}{\partial x_1} (u_{1x_1} u_{3x_1}^2 u_{3x_1 t}) + 4\xi_k I_{00} \frac{\partial}{\partial x_1} (u_{3x_1}^3 u_{30x_1} u_{3x_1 t}) + \xi_k I_{00} \frac{\partial}{\partial x_1} (u_{3x_1}^4 u_{3x_1 t}) \\
& -8C_T I_{00} \frac{\partial}{\partial x_1} (u_{1x_1} u_{30x_1}) - 8C_T I_{00} \frac{\partial}{\partial x_1} (u_{3x_1} u_{30x_1}^2) + 8C_T I_{44} u_{3x_1 x_1 x_1} \\
& -8C_T I_{55} u_{3x_1 x_1} + 8C_T I_{66} \phi_{x_1 x_1} - 8C_T I_{55} \phi_{x_1}
\end{aligned}$$

$$\begin{aligned}
& +12C_T I_{00} \frac{\partial}{\partial x_1} (u_{1x_1}^2 u_{30x_1}) - 8C_T I_{77} \frac{\partial}{\partial x_1} (u_{1x_1} u_{3x_1}) \\
& +24C_T I_{00} \frac{\partial}{\partial x_1} (u_{1x_1} u_{3x_1} u_{30x_1}^2) - 24C_T I_{44} \frac{\partial^2}{\partial x_1^2} (u_{1x_1} u_{3x_1 x_1}) \\
& -24C_T I_{66} \frac{\partial^2}{\partial x_1^2} (u_{1x_1} \phi_{x_1}) + 8C_T I_{55} \frac{\partial}{\partial x_1} (u_{1x_1} \phi) - 12C_T I_{77} \frac{\partial}{\partial x_1} (u_{3x_1}^2 u_{30x_1}) + 12C_T I_{00} \frac{\partial}{\partial x_1} (u_{3x_1}^2 u_{30x_1}^3) \\
& +12C_T I_{44} \frac{\partial}{\partial x_1} (u_{3x_1 x_1}^2 u_{30x_1}) - 24C_T I_{44} \frac{\partial^2}{\partial x_1^2} (u_{3x_1} u_{3x_1 x_1} u_{30x_1}) + 24C_T I_{66} \frac{\partial}{\partial x_1} (u_{3x_1 x_1} \phi_{x_1} u_{30x_1}) \\
& +16C_T I_{55} \frac{\partial}{\partial x_1} (u_{3x_1} \phi u_{30x_1}) - 24C_T I_{66} \frac{\partial^2}{\partial x_1^2} (u_{3x_1} \phi_{x_1} u_{30x_1}) \\
& +12C_T I_{99} \frac{\partial}{\partial x_1} (\phi_{x_1}^2 u_{30x_1}) + 4C_T I_{55} \frac{\partial}{\partial x_1} (\phi^2 u_{30x_1}) \\
& +12C_T I_{00} \frac{\partial}{\partial x_1} (u_{1x_1}^2 u_{3x_1}) + 36C_T I_{00} \frac{\partial}{\partial x_1} (u_{1x_1} u_{3x_1}^2 u_{30x_1}) \\
& -4C_T I_{88} \frac{\partial}{\partial x_1} (u_{3x_1}^3) + 24C_T I_{00} \frac{\partial}{\partial x_1} (u_{3x_1}^3 u_{30x_1}^2) \\
& +12C_T I_{44} \frac{\partial}{\partial x_1} (u_{3x_1} u_{3x_1 x_1}^2) - 12C_T I_{44} \frac{\partial^2}{\partial x_1^2} (u_{3x_1}^2 u_{3x_1 x_1}) \\
& +24C_T I_{66} \frac{\partial}{\partial x_1} (u_{3x_1} u_{3x_1 x_1} \phi_{x_1}) + 12C_T I_{55} \frac{\partial}{\partial x_1} (u_{3x_1}^2 \phi) \\
& -12C_T I_{66} \frac{\partial^2}{\partial x_1^2} (u_{3x_1}^2 \phi_{x_1}) + 12C_T I_{99} \frac{\partial}{\partial x_1} (u_{3x_1} \phi_{x_1}^2) \\
& +4C_T I_{55} \frac{\partial}{\partial x_1} (u_{3x_1} \phi^2) + 12C_T I_{00} \frac{\partial}{\partial x_1} (u_{1x_1} u_{3x_1}^3) \\
& +15C_T I_{00} \frac{\partial}{\partial x_1} (u_{30x_1} u_{3x_1}^4) + 3C_T I_{00} \frac{\partial}{\partial x_1} (u_{3x_1}^5) = F \cos(\omega t), \tag{B.2}
\end{aligned}$$

$$\begin{aligned}
& \rho I_{66} u_{3x_1 t t} + \rho I_{99} \phi_{t t} - \xi_k I_{66} u_{3x_1 x_1 x_1 t} + \frac{1}{2} \xi_k I_{55} u_{3x_1 t} - \xi_k I_{99} \phi_{x_1 x_1 t} \\
& + \frac{1}{2} \xi_k I_{55} \phi_t + 2\xi_k I_{66} \frac{\partial}{\partial x} (u_{3x_1 x_1} u_{1x_1 t}) \\
& - \xi_k I_{55} u_{3x_1} u_{1x_1 t} + 2\xi_k I_{99} \frac{\partial}{\partial x} (\phi_{x_1} u_{1x_1 t}) - \xi_k I_{55} \phi u_{1x_1 t} \\
& + 2\xi_k I_{66} \frac{\partial}{\partial x} (u_{1x_1} u_{3x_1 x_1 t}) + 2\xi_k I_{66} \frac{\partial}{\partial x} (u_{3x_1 x_1} u_{30x_1} u_{3x_1 t}) \\
& - \xi_k I_{55} u_{3x_1} u_{30x_1} u_{3x_1 t} + 2\xi_k I_{99} \frac{\partial}{\partial x} (\phi_x u_{30x_1} u_{3x_1 t}) - \xi_k I_{55} \phi u_{30x_1} u_{3x_1 t} + 2\xi_k I_{99} \frac{\partial}{\partial x} (u_{1x_1} \phi_{x_1 t}) \\
& + 2\xi_k I_{99} \frac{\partial}{\partial x} (u_{3x_1} u_{30x_1} \phi_{x_1 t}) + 2\xi_k I_{66} \frac{\partial}{\partial x} (u_{3x_1} u_{3x_1 x_1} u_{3x_1 t}) \\
& + \xi_k I_{66} \frac{\partial}{\partial x} (u_{3x_1}^2 u_{3x_1 x_1 t}) + 2\xi_k I_{66} \frac{\partial}{\partial x} (u_{3x_1} u_{30x_1} u_{3x_1 x_1 t}) \\
& - \xi_k I_{55} u_{3x_1}^2 u_{3x_1 t} + 2\xi_k I_{99} \frac{\partial}{\partial x} (u_{3x_1} \phi_{x_1} u_{3x_1 t}) - \xi_k I_{55} u_{3x_1} \phi u_{3x_1 t} \\
& + \xi_k I_{99} \frac{\partial}{\partial x} (u_{3x_1}^2 \phi_{x_1 t}) - 8C_T I_{66} u_{3x_1 x_1 x_1} + 8C_T I_{55} u_{3x_1} \\
& - 8C_T I_{99} \phi_{x_1 x_1} + 8C_T I_{55} \phi + 24C_T I_{66} \frac{\partial}{\partial x_1} (u_{1x_1} u_{3x_1 x_1}) \\
& - 8C_T I_{55} u_{1x_1} u_{3x_1} + 24C_T I_{99} \frac{\partial}{\partial x_1} (u_{1x_1} \phi_{x_1}) - 8C_T I_{55} u_{1x_1} \phi \\
& + 24C_T I_{66} \frac{\partial}{\partial x_1} (u_{3x_1} u_{3x_1 x_1} u_{30x_1}) - 8C_T I_{55} u_{3x_1}^2 u_{30x_1} \\
& + 24C_T I_{99} \frac{\partial}{\partial x_1} (u_{3x_1} \phi_{x_1} u_{30x_1}) - 8C_T I_{55} u_{3x_1} \phi u_{30x_1}
\end{aligned}$$

$$+12C_T I_{66} \frac{\partial}{\partial x_1} \left(u_{3x_1}^2 u_{3x_1 x_1} \right) - 4C_T I_{55} u_{3x_1}^3 + 12C_T I_{99} \frac{\partial}{\partial x_1} \left(u_{3x_1}^2 \phi_{x_1} \right) - 4C_T I_{55} u_{3x_1}^2 \phi = 0. \quad (\text{B.3})$$

Appendix C

$$C_{11}^{NL} : +2\xi_k I_{00} \frac{1}{\eta} \int_0^1 U_l(x_1) \frac{d}{dx_1} \left(U_i'(x_1) U_j'(x_1) \right) dx, \quad (\text{C.1})$$

$$C_{12}^{NL} : +2\xi_k I_{00} \int_0^1 U_l(x_1) \frac{d}{dx_1} \left(U_i'(x_1) W_j'(x_1) W_0'(x_1) \right) dx, \quad (\text{C.2})$$

$$C_{13}^{NL} : +2\xi_k I_{00} \int_0^1 U_l(x_1) \frac{d}{dx_1} \left(U_i'(x_1) W_j'(x_1) W_0'(x_1) \right) dx_1, \quad (\text{C.3})$$

$$C_{14}^{NL} : -\xi_k I_{77} \frac{1}{\eta} \int_0^1 U_l(x_1) \frac{d}{dx_1} \left(W_i'(x_1) W_j'(x_1) \right) dx_1 \\ + 2\xi_k \eta \int_0^1 U_l(x_1) \frac{d}{dx_1} \left(W_i''(x_1) W_j''(x_1) \right) dx_1 \\ + 2\xi_k I_{00} \eta \int_0^1 U_l(x_1) \frac{d}{dx_1} \left(W_i'(x_1) W_j'(x_1) W_0'^2(x_1) \right) dx_1, \quad (\text{C.4})$$

$$C_{15}^{NL} : +2\xi_k I_{66} \int_0^1 U_l(x_1) \frac{d}{dx_1} \left(W_i''(x_1) \psi_j'(x_1) \right) dx_1 \\ + \xi_k I_{55} \frac{1}{\eta^2} \int_0^1 U_l(x_1) \frac{d}{dx_1} \left(W_i'(x_1) \psi_j(x_1) \right) dx_1, \quad (\text{C.5})$$

$$C_{16}^{NL} : +2\xi_k I_{66} \int_0^1 U_l(x_1) \frac{d}{dx_1} \left(W_i''(x_1) \psi_j'(x_1) \right) dx_1 \\ + \xi_k I_{55} \frac{1}{\eta^2} \int_0^1 U_l(x_1) \frac{d}{dx_1} \left(W_i'(x_1) \psi_j(x_1) \right) dx_1, \quad (\text{C.6})$$

$$C_{17}^{NL} : +2\xi_k I_{99} \frac{1}{\eta} \int_0^1 U_l(x_1) \frac{d}{dx_1} \left(\psi_i'(x_1) \psi_j'(x_1) \right) dx_1 \\ + \xi_k I_{55} \frac{1}{\eta^3} \int_0^1 U_l(x_1) \frac{d}{dx_1} \left(\psi_i(x_1) \psi_j(x_1) \right) dx_1, \quad (\text{C.7})$$

$$C_{18}^{NL} : +\xi_k I_{00} \int_0^1 U_l(x_1) \frac{d}{dx_1} \left(U_i'(x_1) W_j'(x_1) W_k'(x_1) \right) dx_1, \quad (\text{C.8})$$

$$C_{19}^{NL} : +2\xi_k I_{00} \int_0^1 U_l(x_1) \frac{d}{dx_1} \left(U_i'(x_1) W_j'(x_1) W_k'(x_1) \right) dx_1, \quad (C.9)$$

$$C_{110}^{NL} : +3\xi_k I_{00} \eta \int_0^1 U_l(x_1) \frac{d}{dx_1} \left(W_i'(x_1) W_j'(x_1) W_k'(x_1) W_0'(x_1) \right) dx_1, \quad (C.10)$$

$$C_{111}^{NL} : +\xi_k I_{00} \eta \int_0^1 U_l(x_1) \frac{d}{dx_1} \left(W_i'(x_1) W_j'(x_1) W_k'(x_1) W_m'(x_1) \right) dx_1, \quad (C.11)$$

$$C_{21}^{NL} : +2\xi_k I_{00} \int_0^1 W_l(x_1) \frac{d}{dx_1} \left(U_i'(x_1) U_j'(x_1) W_0'(x_1) \right) dx_1, \quad (C.12)$$

$$C_{22}^{NL} : +2\xi_k I_{00} \eta \int_0^1 W_l(x_1) \frac{d}{dx_1} \left(U_i'(x_1) W_j'(x_1) W_0'^2(x_1) \right) dx_1$$

$$- \xi_k I_{77} \frac{1}{\eta} \int_0^1 W_l(x_1) \frac{d}{dx_1} \left(U_i'(x_1) W_j'(x_1) \right) dx_1$$

$$- 2\xi_k I_{00} \eta \int_0^1 W_l(x_1) \frac{d^2}{dx_1^2} \left(U_i'(x_1) W_j''(x_1) \right) dx_1, \quad (C.13)$$

$$C_{23}^{NL} : -2\xi_k I_{66} \int_0^1 W_l(x_1) \frac{d^2}{dx_1^2} \left(U_i'(x_1) \psi_j'(x_1) \right) dx_1$$

$$+ \xi_k I_{55} \frac{1}{\eta^2} \int_0^1 W_l(x_1) \frac{d}{dx_1} \left(U_i'(x_1) \psi_j(x_1) \right) dx_1, \quad (C.14)$$

$$C_{24}^{NL} : +2\xi_k I_{00} \eta \int_0^1 W_l(x_1) \frac{d}{dx_1} \left(U_i'(x_1) W_j'(x_1) W_0'^2(x_1) \right) dx_1$$

$$- 2\xi_k \eta \int_0^1 W_l(x_1) \frac{d^2}{dx_1^2} \left(U_i'(x_1) W_j''(x_1) \right) dx_1, \quad (C.15)$$

$$C_{25}^{NL} : +2\xi_k I_{00} \eta^2 \int_0^1 W_l(x_1) \frac{d}{dx_1} \left(W_i'(x_1) W_j'(x_1) W_0'^3(x_1) \right) dx_1$$

$$+ 2\xi_k \eta^2 \int_0^1 W_l(x_1) \frac{d}{dx_1} \left(W_i''(x_1) W_j''(x_1) W_0'(x_1) \right) dx_1$$

$$- 2\xi_k I_{77} \int_0^1 W_l(x_1) \frac{d}{dx_1} \left(W_i'(x_1) W_j'(x_1) W_0'(x_1) \right) dx_1$$

$$- 2\xi_k \eta^2 \int_0^1 W_l(x_1) \frac{d^2}{dx_1^2} \left(W_i'(x_1) W_j''(x_1) W_0'(x_1) \right) dx_1, \quad (C.16)$$

$$\begin{aligned}
C_{26}^{NL} : & +2\xi_k I_{66}\eta \int_0^1 W_l(x_1) \frac{d}{dx_1} \left(W_i''(x_1) \psi_j'(x_1) W_0'(x_1) \right) dx_1 \\
& +2\xi_k I_{55} \frac{1}{\eta} \int_0^1 W_l(x_1) \frac{d}{dx_1} \left(W_i'(x_1) \psi_j(x_1) W_0'(x_1) \right) dx_1 \\
& -2\xi_k I_{66}\eta \int_0^1 W_l(x_1) \frac{d^2}{dx_1^2} \left(W_i'(x_1) \psi_j'(x_1) W_0'(x_1) \right) dx_1,
\end{aligned} \tag{C.17}$$

$$C_{27}^{NL} : -2\xi_k I_{66} \int_0^1 W_l(x) \frac{d^2}{dx_1^2} \left(U_i'(x_1) \psi_j'(x_1) \right) dx_1, \tag{C.18}$$

$$\begin{aligned}
C_{28}^{NL} : & +2\xi_k I_{66}\eta \int_0^1 W_l(x_1) \frac{d}{dx_1} \left(W_i''(x_1) \psi_j'(x_1) W_0'(x_1) \right) dx_1 \\
& +\xi_k I_{55} \frac{1}{\eta} \int_0^1 W_l(x_1) \frac{d}{dx_1} \left(W_i'(x_1) \psi_j(x_1) W_0'(x_1) \right) dx_1 \\
& -2\xi_k I_{66}\eta \int_0^1 W_l(x_1) \frac{d^2}{dx_1^2} \left(W_i'(x_1) \psi_j'(x_1) W_0'(x_1) \right) dx_1,
\end{aligned} \tag{C.19}$$

$$\begin{aligned}
C_{29}^{NL} : & +2\xi_k I_{99} \int_0^1 W_l(x_1) \frac{d}{dx_1} \left(\psi_i'(x_1) \psi_j'(x_1) W_0'(x_1) \right) dx_1 \\
& +\xi_k I_{55} \frac{1}{\eta^2} \int_0^1 W_l(x_1) \frac{d}{dx_1} \left(\psi_i(x_1) \psi_j(x_1) W_0'(x_1) \right) dx_1,
\end{aligned} \tag{C.20}$$

$$C_{210}^{NL} : +2\xi_k I_{00} \int_0^1 W_l(x_1) \frac{d}{dx_1} \left(U_i'(x_1) U_j'(x_1) W_k'(x_1) \right) dx_1, \tag{C.21}$$

$$C_{211}^{NL} : +3\xi_k I_{00}\eta \int_0^1 W_l(x_1) \frac{d}{dx_1} \left(U_i'(x_1) W_j'(x_1) W_k'(x_1) W_0'(x_1) \right) dx_1, \tag{C.22}$$

$$C_{212}^{NL} : +4\xi_k I_{00}\eta \int_0^1 W_l(x_1) \frac{d}{dx_1} \left(U_i'(x_1) W_j'(x_1) W_k'(x_1) W_0'(x_1) \right) dx_1, \tag{C.23}$$

$$\begin{aligned}
C_{213}^{NL} : & +5\xi_k I_{00}\eta^2 \int_0^1 W_l(x_1) \frac{d}{dx_1} \left(W_i'(x_1) W_j'(x_1) W_k'(x_1) W_0'^2(x_1) \right) dx_1 \\
& -\xi_k I_{88} \int_0^1 W_l(x_1) \frac{d}{dx_1} \left(W_i'(x_1) W_j'(x_1) W_k'(x_1) \right) dx_1 \\
& +2\xi_k \eta^2 \int_0^1 W_l(x_1) \frac{d}{dx_1} \left(W_i'(x_1) W_j''(x_1) W_k''(x_1) \right) dx_1
\end{aligned}$$

$$-3\xi_k \eta^2 \int_0^1 W_l(x_1) \frac{d^2}{dx_1^2} \left(W_i'(x_1) W_j'(x_1) W_k''(x_1) \right) dx_1, \quad (C.24)$$

$$\begin{aligned} C_{214}^{NL} : & +2\xi_k I_{66}\eta \int_0^1 W_l(x_1) \frac{d}{dx_1} \left(W_i'(x_1) W_j''(x_1) \psi_k'(x_1) \right) dx_1 \\ & +2\xi_k I_{55} \frac{1}{\eta} \int_0^1 W_l(x_1) \frac{d}{dx_1} \left(W_i'(x_1) W_j'(x_1) \psi_k(x_1) \right) dx_1 \\ & -2\xi_k I_{66}\eta \int_0^1 W_l(x_1) \frac{d^2}{dx_1^2} \left(W_i'(x_1) W_j'(x_1) \psi_k'(x_1) \right) dx_1, \end{aligned} \quad (C.25)$$

$$\begin{aligned} C_{215}^{NL} : & +2\xi_k I_{66}\eta \int_0^1 W_l(x_1) \frac{d}{dx_1} \left(W_i'(x_1) W_j''(x_1) \psi_k'(x_1) \right) dx_1 \\ & +\xi_k I_{55} \frac{1}{\eta} \int_0^1 W_l(x_1) \frac{d}{dx_1} \left(W_i'(x_1) W_j'(x_1) \psi_k(x_1) \right) dx_1 \\ & -\xi_k I_{66}\eta \int_0^1 W_l(x_1) \frac{d^2}{dx_1^2} \left(W_i'(x_1) W_j'(x_1) \psi_k'(x_1) \right) dx_1, \end{aligned} \quad (C.26)$$

$$\begin{aligned} C_{216}^{NL} : & +2\xi_k I_{99} \int_0^1 W_l(x_1) \frac{d}{dx_1} \left(W_i'(x_1) \psi_j'(x_1) \psi_k'(x_1) \right) dx_1 \\ & +\xi_k I_{55} \frac{1}{\eta^2} \int_0^1 W_l(x_1) \frac{d}{dx_1} \left(W_i'(x_1) \psi_j(x_1) \psi_k(x_1) \right) dx_1, \end{aligned} \quad (C.27)$$

$$C_{217}^{NL} : +\xi_k I_{00}\eta \int_0^1 W_l(x_1) \frac{d}{dx_1} \left(U_i'(x_1) W_j'(x_1) W_k'(x_1) W_m'(x_1) \right) dx_1, \quad (C.28)$$

$$C_{218}^{NL} : +2\xi_k I_{00}\eta \int_0^1 W_l(x_1) \frac{d}{dx_1} \left(U_i'(x_1) W_j'(x_1) W_k'(x_1) W_m'(x_1) \right) dx_1, \quad (C.29)$$

$$C_{219}^{NL} : +4\xi_k I_{00}\eta^2 \int_0^1 W_l(x_1) \frac{d}{dx_1} \left(W_i'(x_1) W_j'(x_1) W_k'(x_1) W_m'(x_1) W_0'(x_1) \right) dx_1, \quad (C.30)$$

$$C_{220}^{NL} : +\xi_k I_{00}\eta^2 \int_0^1 W_l(x_1) \frac{d}{dx_1} \left(W_i'(x_1) W_j'(x_1) W_k'(x_1) W_m'(x_1) W_n'(x_1) \right) dx_1, \quad (C.31)$$

$$C_{31}^{NL} : +2\xi_k I_{66}\eta^2 \int_0^1 \psi_l(x_1) \frac{d}{dx_1} \left(U_j'(x_1) W_j''(x_1) \right) dx_1 - \xi_k I_{55} \int_0^1 \psi_l(x_1) U_i'(x_1) W_j'(x_1) dx_1, \quad (C.32)$$

$$C_{32}^{NL} : +2\xi_k I_{99}\eta \int_0^1 \psi_l(x_1) \frac{d}{dx_1} \left(U_i'(x_1) \psi_j'(x_1) \right) dx_1 - \xi_k I_{55} \frac{1}{\eta} \int_0^1 \psi_l(x_1) U_i'(x_1) \psi_j(x_1) dx_1, \quad (C.33)$$

$$C_{33}^{NL} : +2\xi_k I_{66}\eta^2 \int_0^1 \psi_l(x_1) \frac{d}{dx_1} \left(U_j'(x_1) W_j''(x_1) \right) dx_1, \quad (C.34)$$

$$C_{34}^{NL} : +4\xi_k I_{66}\eta^3 \int_0^1 \psi_l(x_1) \frac{d}{dx_1} \left(W_i'(x_1) W_j''(x_1) W_0'(x_1) \right) dx_1 \\ - \xi_k I_{55}\eta \int_0^1 \psi_l(x_1) W_i'(x_1) W_j'(x_1) W_0'(x_1) dx_1, \quad (C.35)$$

$$C_{35}^{NL} : +2\xi_k I_{99}\eta^2 \int_0^1 \psi_l(x_1) \frac{d}{dx_1} \left(W_i'(x_1) \psi_i'(x_1) W_0'(x_1) \right) dx_1 \\ - \xi_k I_{55} \int_0^1 \psi_l(x_1) W_i'(x_1) \psi_i(x_1) W_0'(x_1) dx_1, \quad (C.36)$$

$$C_{36}^{NL} : +2\xi_k I_{99}\eta \int_0^1 \psi_l(x_1) \frac{d}{dx_1} \left(U_i'(x_1) \psi_j'(x_1) \right) dx_1, \quad (C.37)$$

$$C_{37}^{NL} : +2\xi_k I_{99}\eta^2 \int_0^1 \psi_l(x_1) \frac{d}{dx_1} \left(W_i'(x_1) \psi_i'(x_1) W_0'(x_1) \right) dx_1, \quad (C.38)$$

$$C_{38}^{NL} : +3\xi_k I_{66}\eta^3 \int_0^1 \psi_l(x_1) \frac{d}{dx_1} \left(W_i'(x_1) W_j'(x_1) W_k''(x_1) \right) dx_1 \\ - \xi_k I_{55}\eta \int_0^1 \psi_l(x_1) W_i'(x_1) W_j'(x_1) W_k'(x_1) dx_1, \quad (C.39)$$

$$C_{39}^{NL} : +2\xi_k I_{99}\eta^2 \int_0^1 \psi_l(x_1) \frac{d}{dx_1} \left(W_i'(x_1) W_j'(x_1) \psi_k'(x_1) \right) dx_1 \\ - \xi_k I_{55} w_x \phi w_{xt} \int_0^1 \psi_l(x_1) W_i'(x_1) W_j'(x_1) \psi_k(x_1) dx_1, \quad (C.40)$$

$$C_{310}^{NL} : +\xi_k I_{99}\eta^2 \int_0^1 \psi_l(x_1) \frac{d}{dx_1} \left(W_i'(x_1) W_j'(x_1) \psi_k'(x_1) \right) dx_1, \quad (C.41)$$

References

1. Yu, L., Zhang, D., Fang, Q., Cao, L., Xu, T., Li, Q.: Surface settlement of subway station construction using pile-beam-arch approach. *Tunn. Undergr. Space Technol.* **90**, 340–356 (2019)
2. Li, B., Wang, Z.: Numerical study on the response of ground movements to construction activities of a metro station using the pile-beam-arch method. *Tunn. Undergr. Space Technol.* **88**, 209–220 (2019)
3. Chen, X., Zhang, X., Wang, L., Chen, L.: An arch-linear composed beam piezoelectric energy harvester with magnetic coupling: design, modeling and dynamic analysis. *J. Sound Vib.* **513**, 116394 (2021)
4. Zhang, X., Chen, L., Chen, X., Zhu, F., Guo, Y.: Time-domain dynamic characteristics analysis and experimental research of tri-stable piezoelectric energy harvester. *Micromachines* **12**, 1045 (2021)
5. Tzou, H., Zhang, X.: A flexoelectric double-curvature nonlinear shell energy harvester. *J. Vib. Acoust.* **138**, 031006 (2016)

6. Zhang, X., Zuo, M., Yang, W., Wan, X.: A tri-stable piezoelectric vibration energy harvester for composite shape beam: nonlinear modeling and analysis. *Sensors* **20**, 1370 (2020)
7. Yang, Z., Wang, Y.Q., Zuo, L., Zu, J.: Introducing arc-shaped piezoelectric elements into energy harvesters. *Energy Convers. Manag.* **148**, 260–266 (2017)
8. Hafiz, M.A.A., Kosuru, L., Ramini, A., Chappanda, K.N., Younis, M.I.: In-plane MEMS shallow arch beam for mechanical memory. *Micromachines* **7**, 191 (2016)
9. Liu, N., Plucinsky, P., Jeffers, A.E.: Combining load-controlled and displacement-controlled algorithms to model thermal-mechanical snap-through instabilities in structures. *J. Eng. Mech.* **143**, 04017051 (2017)
10. Zhao, B., Long, C., Peng, X., Chen, J., Liu, T., Zhang, Z., Lai, A.: Size effect and geometrically nonlinear effect on thermal post-buckling of micro-beams: a new theoretical analysis. *Contin. Mech. Thermodyn.* **34**, 519–532 (2022)
11. Liu, N., Jeffers, A.E.: Adaptive isogeometric analysis in structural frames using a layer-based discretization to model spread of plasticity. *Comput. Struct.* **196**, 1–11 (2018)
12. Liu, N., Jeffers, A.E.: Isogeometric analysis of laminated composite and functionally graded sandwich plates based on a layerwise displacement theory. *Compos. Struct.* **176**, 143–153 (2017)
13. Liu, N., Jeffers, A.E.: A geometrically exact isogeometric Kirchhoff plate: feature-preserving automatic meshing and C 1 rational triangular Bézier spline discretizations. *Int. J. Numer. Methods Eng.* **115**, 395–409 (2018)
14. Surana, K., Mysore, D., Reddy, J.: Thermodynamic consistency of beam theories in the context of classical and non-classical continuum mechanics and a thermodynamically consistent new formulation. *Contin. Mech. Thermodyn.* **31**, 1283–1312 (2019)
15. Malikan, M., Wiczenbach, T., Eremeyev, V.A.: Thermal buckling of functionally graded piezomagnetic micro-and nanobeams presenting the flexomagnetic effect. *Contin. Mech. Thermodyn.* **34**, 1051–1066 (2022)
16. Liu, N., Ren, X., Lua, J.: An isogeometric continuum shell element for modeling the nonlinear response of functionally graded material structures. *Compos. Struct.* **237**, 111893 (2020)
17. Liu, N., Johnson, E.L., Rajanna, M.R., Lua, J., Phan, N., Hsu, M.-C.: Blended isogeometric Kirchhoff–Love and continuum shells. *Comput. Methods Appl. Mech. Eng.* **385**, 114005 (2021)
18. Cazzani, A., Malagù, M., Turco, E.: Isogeometric analysis: a powerful numerical tool for the elastic analysis of historical masonry arches. *Contin. Mech. Thermodyn.* **28**, 139–156 (2016)
19. de Leo, A.M., Contento, A., Di Egidio, A.: Semi-analytical approach for the study of linear static behaviour and buckling of shells with single constant curvature. *Contin. Mech. Thermodyn.* **27**, 767–785 (2015)
20. Liu, N., Lua, J., Rajanna, M.R., Johnson, E., Hsu, M.-C., Phan, N.D.: Buffet-induced structural response prediction of aircraft horizontal stabilizers based on immersogeometric analysis and an isogeometric blended shell approach. In: *AIAA SCITECH 2022 Forum*, p. 0852 (2022)
21. Liu, N., Hsu, M.-C., Lua, J., Phan, N.: A large deformation isogeometric continuum shell formulation incorporating finite strain elastoplasticity. *Comput. Mech.* **70**, 965–976 (2022)
22. Chróścielewski, J., Schmidt, R., Eremeyev, V.A.: Nonlinear finite element modeling of vibration control of plane rod-type structural members with integrated piezoelectric patches. *Contin. Mech. Thermodyn.* **31**, 147–188 (2019)
23. Liu, N., Rajanna, M.R., Johnson, E.L., Lua, J., Phan, N., Hsu, M.-C.: Isogeometric blended shells for dynamic analysis: simulating aircraft takeoff and the resulting fatigue damage on the horizontal stabilizer. *Comput. Mech.* **70**, 1013–1024 (2022)
24. Yang, Z., Zhao, S., Yang, J., Lv, J., Liu, A., Fu, J.: In-plane and out-of-plane free vibrations of functionally graded composite arches with graphene reinforcements. *Mech. Adv. Mater. Struct.* **28**, 2046–2056 (2021)
25. Zhao, S., Yang, Z., Kitipornchai, S., Yang, J.: Dynamic instability of functionally graded porous arches reinforced by graphene platelets. *Thin-Walled Struct.* **147**, 106491 (2020)
26. Ghayesh, M.H., Farokhi, H.: Mechanics of tapered axially functionally graded shallow arches. *Compos. Struct.* **188**, 233–241 (2018)
27. Farokhi, H., Ghayesh, M.H., Hussain, S.: Pull-in characteristics of electrically actuated MEMS arches. *Mech. Mach. Theory* **98**, 133–150 (2016)
28. Baccocchi, M., Tarantino, A.M.: Bending of hyperelastic beams made of transversely isotropic material in finite elasticity. *Appl. Math. Modell.* **100**, 55–76 (2021)
29. Du, P., Dai, H.-H., Wang, J., Wang, Q.: Analytical study on growth-induced bending deformations of multi-layered hyperelastic plates. *Int. J. Non-Linear Mech.* **119**, 103370 (2020)
30. Baccocchi, M., Tarantino, A.M.: Finite bending of hyperelastic beams with transverse isotropy generated by longitudinal porosity. *Eur. J. Mech. A Solids* **85**, 104131 (2021)
31. Herrmann, H.: A constitutive model for linear hyperelastic materials with orthotropic inclusions by use of quaternions. *Contin. Mech. Thermodyn.* **33**, 1375–1384 (2021)
32. Breslavsky, I.D., Amabili, M., Legrand, M.: Nonlinear vibrations of thin hyperelastic plates. *J. Sound Vib.* **333**, 4668–4681 (2014)
33. Amabili, M., Breslavsky, I., Reddy, J.: Nonlinear higher-order shell theory for incompressible biological hyperelastic materials. *Comput. Methods Appl. Mech. Eng.* **346**, 841–861 (2019)
34. Amabili, M., Balasubramanian, P., Breslavsky, I.D., Ferrari, G., Garziera, R., Riabova, K.: Experimental and numerical study on vibrations and static deflection of a thin hyperelastic plate. *J. Sound Vib.* **385**, 81–92 (2016)
35. Breslavsky, I.D., Amabili, M., Legrand, M.: Static and dynamic behavior of circular cylindrical shell made of hyperelastic arterial material. *J. Appl. Mech.* **83**, 051002 (2016)
36. Lanzoni, L., Tarantino, A.M.: Finite anticlastic bending of hyperelastic solids and beams. *J. Elast.* **131**, 137–170 (2018)
37. Lanzoni, L., Tarantino, A.M.: Nonuniform bending theory of hyperelastic beams in finite elasticity. *Int. J. Non-Linear Mech.* **135**, 103765 (2021)
38. Lanzoni, L., Tarantino, A.M.: The bending of beams in finite elasticity. *J. Elast.* **139**, 91–121 (2020)
39. Khaniki, H.B., Ghayesh, M.H., Chin, R., Chen, L.-Q.: Experimental characteristics and coupled nonlinear forced vibrations of axially travelling hyperelastic beams. *Thin-Walled Struct.* **170**, 108526 (2022)

40. Khaniki, H.B., Ghayesh, M.H., Chin, R., Hussain, S.: Nonlinear continuum mechanics of thick hyperelastic sandwich beams using various shear deformable beam theories. *Contin. Mech. Thermodyn.* **34**, 781–827 (2022)
41. Khaniki, H.B., Ghayesh, M.H., Chin, R., Amabili, M.: Large amplitude vibrations of imperfect porous-hyperelastic beams via a modified strain energy. *J. Sound Vib.* **513**, 116416 (2021)
42. Khaniki, H.B., Ghayesh, M.H., Chin, R., Amabili, M.: A review on the nonlinear dynamics of hyperelastic structures. *Nonlinear Dyn.* **110**, 963–994 (2022)
43. Altmeyer, G., Panicaud, B., Rouhaud, E., Wang, M., Roos, A., Kerner, R.: Viscoelasticity behavior for finite deformations, using a consistent hypoelastic model based on Rivlin materials. *Contin. Mech. Thermodyn.* **28**, 1741–1758 (2016)
44. Menga, N., Bottiglione, F., Carbone, G.: Nonlinear viscoelastic isolation for seismic vibration mitigation. *Mech. Syst. Signal Process.* **157**, 107626 (2021)
45. Penas, R., Balmes, E., Gaudin, A.: A unified non-linear system model view of hyperelasticity, viscoelasticity and hysteresis exhibited by rubber. *Mech. Syst. Signal Process.* **170**, 108793 (2022)
46. Huang, Y., Oterkus, S., Hou, H., Oterkus, E., Wei, Z., Zhang, S.: Peridynamic model for visco-hyperelastic material deformation in different strain rates. *Contin. Mech. Thermodyn.* **34**, 977–1011 (2019)
47. Buchen, S., Kröger, N.H., Reppel, T., Weinberg, K.: Time-dependent modeling and experimental characterization of foamed EPDM rubber. *Contin. Mech. Thermodyn.* **33**, 1747–1764 (2021)
48. Li, L., Maccabi, A., Abiri, A., Juo, Y.-Y., Zhang, W., Chang, Y.-J., Saddik, G.N., Jin, L., Grundfest, W.S., Dutson, E.P.: Characterization of perfused and sectioned liver tissue in a full indentation cycle using a visco-hyperelastic model. *J. Mech. Behav. Biomed. Mater.* **90**, 591–603 (2019)
49. Amabili, M.: *Nonlinear Vibrations and Stability of Shells and Plates*. Cambridge University Press (2008)
50. Bower, A.F.: *Applied Mechanics of Solids*. CRC Press (2009)
51. Rivlin, R.: Large elastic deformations of isotropic materials VI. Further results in the theory of torsion, shear and flexure. *Philos. Trans. R. Soc. Lond. Ser. A Math. Phys. Sci.* **242**, 173–195 (1949)
52. Mooney, M.: A theory of large elastic deformation. *J. Appl. Phys.* **11**, 582–592 (1940)
53. Xiang, H., Yang, J.: Free and forced vibration of a laminated FGM Timoshenko beam of variable thickness under heat conduction. *Compos. Part B Eng.* **39**, 292–303 (2008)
54. Reddy, J.N.: *Mechanics of Laminated Composite Plates and Shells: Theory and Analysis*. CRC Press (2003)
55. Fukahori, Y., Seki, W.: Molecular behaviour of elastomeric materials under large deformation: 1. Re-evaluation of the Mooney–Rivlin plot. *Polymer* **33**, 502–508 (1992)
56. ANSYS®Multiphysics™, Workbench 19.2, Workbench User’s Guide, ANSYS Workbench Systems, Analysis Systems, Static Structural
57. Meyers, M.A., Chawla, K.K.: *Mechanical Behavior of Materials*. Cambridge University Press (2008)